Chemical Catalysis of Electrochemical Reactions. Homogeneous Catalysis of the Electrochemical Reduction of Carbon Dioxide by Iron("0") Porphyrins. Role of the Addition of Magnesium Cations

Mohamed Hammouche,[1a] Doris Lexa,[1a] Michel Momenteau,[1b] and Jean-Michel Savéant*,[1a]

Contribution from the Laboratoire d'Electrochimie Moléculaire de l'Université de Paris 7, Unité Associée au CNRS N° 438, 2 place Jussieu, 75251 Paris Cedex 05, France, and the Institut Curie, Section de Biologie, Unité Inserm 219, 91405 Orsay, France. *Received March 4, 1991*

Abstract: Iron("0") porphyrins catalyze the electrochemical reduction of CO_2. The main reduction product is CO. In DMF, with tetraalkylammonium salts as supporting electrolyte, the porphyrin is however destroyed by carboxylation and/or hydrogenation of the ring after a few catalytic cycles. The presence of a hard electrophile such as Mg^{2+} ion dramatically improves the rate of the reaction, the production of CO, and, most importantly, the stability of the catalyst. The reaction mechanism involves the introduction of one molecule of CO_2 into the iron coordination sphere. The addition of a second molecule of CO_2 acts as a Lewis acid and then allows the breaking of one C–O bond of the first CO_2 molecule thus leading to CO. This process is accelerated by Mg^{2+} ions in a way that depends upon the temperature. At low temperatures (–40 °C), the Mg^{2+} ions facilitate the decomposition of the complex containing two molecules of CO_2, whereas, at room temperature, Mg^{2+} ions triggers the breaking of the bond at the level of the complex containing a single molecule of CO_2 in its coordination sphere. The combined action of iron("0") porphyrins and of Mg^{2+} ions offers a remarkable example of a bimetallic catalysis where an electron-rich center starts the reduction process and an electron-deficient center assists the transformation of the bond system.

The electrochemical reduction of carbon dioxide has attracted considerable attention as a possible source of carbon for the synthesis of organic molecules and as a possible means of energy storage. CO_2 is a low-energy molecule, and its electrochemical reduction into its anion radical requires a quite negative potential.[2] The products of the direct electrochemical reduction depend both on the electrode and the reaction medium. In low acidity solvents, such as *N,N'*-dimethylformamide (DMF), and with inert electrodes, such as mercury and lead, the reduction takes place at potential slightly negative to the standard potential of the $CO_2/CO_2^{\bullet-}$ couple. This indicates that the interactions between the electrode on the one hand and the reactant, intermediates, and products on the other hand are weak. In other words, the electrode functions as a heterogeneous outer-sphere electron donor. Under these conditions, three products, oxalate, formate, and carbon monoxide, are formed[3a-c] according to the following mechanism.[3d-i]

$$CO_2 + e^- \rightleftharpoons CO_2^{\bullet-}$$

$$CO_2^{\bullet-} + H_2O \text{ (residual or added)} \longrightarrow {}^{\bullet}CO_2H$$

$${}^{\bullet}CO_2H + CO_2^{\bullet-} \longrightarrow CO_2 + HCO_2^-$$

$$2CO_2^{\bullet-} \longrightarrow {}^-O_2C\text{-}CO_2^-$$

$$CO_2^{\bullet-} + CO_2 \longrightarrow O{=}\dot{C}\text{-}O\text{-}C(=O)O^-$$

$$O{=}\dot{C}\text{-}O\text{-}C(=O)O^- + CO_2^{\bullet-} \longrightarrow CO + CO_3^{2-}$$

In water, the main product is formic acid as discovered a long time ago[4a-c] and confirmed by more recent studies.[4d] However, the product distribution considerably depends upon the nature of the electrode material and of the reaction medium.[5] Chemisorption of intermediates and/or products most probably play a cruxial role.[6] The metal then plays the role of a heterogeneous

(1) (a) Université de Paris 7. (b) Institut Curie.

(2) (a) The standard potential of the $CO_2/CO_2^{\bullet-}$ couple in *N,N'*-dimethylformamide (DMF) with 0.1 M NEt_4ClO_4 as supporting electrolyte has been estimated to be −2.2 V vs SCE by cyclic voltammetry on a mercury electrode.[2b] More recent results obtained by means of redox catalysis[2c,d] indicate a somewhat more negative value that depends upon the nature of the solvent and the nature and concentration of the supporting electrolyte.[2c] It may also depend upon the CO_2 concentration in view of possible acid–base interactions between CO_2 and $CO_2^{\bullet-}$. (b) Lamy, E.; Nadjo, L.; Savéant, J.-M. *J. Electroanal. Chem.* **1977**, *78*, 403. (c) Andrieux, C. P.; Savéant, J.-M. Electrochemical Reactions. In *Investigations of Rates and Mechanisms*; Bernasconi, C. F., Ed.; Wiley: New York, 1986; Vol. 6, 4/E, Part 2, p 305. (d) Andrieux, C. P.; Hapiot, P.; Savéant, J.-M. *Chem. Rev.* **1990**, *90*, 723. (e) Vianello, E., private communication, 1990.

(3) (a) Kaiser, U.; Heitz, E. *Ber. Bunsenges. Phys. Chem.* **1973**, *77*, 818. (b) Gressin, J. C.; Michelet, D.; Nadjo, L.; Savéant, J.-M. *Nouv. J. Chim.* **1979**, *3*, 545. (c) Formate comes from the reaction of the CO_2 anion radical with the water contained in the solvent. Oxalate prevails at high current densities. It results from the coupling of two anion radicals. CO is obtained at low current densities and high concentrations of CO_2. Interestingly for the following discussion, CO results from an acid–base reaction where CO_2 plays the role of the acid and is responsible for the breaking of one C–O bond in the anion radical. It is possible to favor, in accord with the preceding mechanism, the production of oxalate up to quantitative yields which have been achieved on the pilot scale.[3g] (d) Amatore, C.; Savéant, J.-M. *J. Am. Chem. Soc.* **1981**, *103*, 5021. (e) Amatore, C.; Savéant, J.-M. *J. Electroanal. Chem.* **1981**, *125*, 22. (f) Amatore, C.; Nadjo, L.; Savéant, J.-M. *Nouv. J. Chim.* **1984**, *8*, 565. (g) Fisher, J.; Lehmann, T.; Heitz, E. *J. Appl. Electrochem.* **1981**, *11*, 743. (h) In contrast, on platinum, CO is the sole product in DMF and is formed with an excellent faradaic yield.[2e] The same is true for Au, Sn, Cd, and Zn layers freshly deposited on the electrode surface in DMF or *N*-methylpyrrolidone.[3i] (i) Massebieau, M. C.; Dunach, E.; Troupel, M.; Périchon, J. *New J. Chem.* **1990**, *14*, 259.

(4) (a) Royer, M. E. *C. R. Acad. Sci.* **1870**, *70*, 731. (b) Cohen, A.; Jahn, S. *Ber. Dtsch. Chem. Ges.* **1904**, *37*, 2836. (c) Ehrenfeld, R. *Ber. Dtsch. Chem. Ges.* **1905**, *38*, 4138. (d) Russel, P. G.; Kovac, N.; Srinivasan, S.; Steinberg, M. *J. Electrochem. Soc.* **1977**, *124*, 1329.

(5) Besides formate and CO,[5b,c] other products such as formaldehyde,[5d] methanol,[5e,f] and methane[5f-k] can be formed. It is however interesting to note that on an inert electrode such as lead, one obtains, with a large overpotential, solely formate,[5l] as expected from the results obtained in DMF. On the other hand, oxalate, partially reduced into glyoxalate, is formed, together with formate, on mercury in the presence of quaternary ammonium salts, again with a large overpotential.[5m] (b) Hori, Y.; Kikuchi, K.; Suzuki, S. *Chem. Lett.* **1985**, 1695. (c) Hori, Y.; Murata, A.; Kikuchi, K.; Suzuki, S. *J. Chem. Soc.,Chem. Commun.* **1987**, 728. (d) Osetrova, N. V.; Vasiliev, Yu. B.; Bagotskii, V. S.; Sadkova, R. G.; Cherashev, A. F.; Khrushch, A. P. *Elektrokhimiya* **1984**, *20*, 286. (e) Summers, D. P.; Leach, S.; Frese, K. W. *J. Electroanal. Chem.* **1986**, *205*, 219. (f) Frese, K. W.; Leach, S. *J. Electrochem. Soc.* **1985**, *132*, 259. (g) Hori, Y.; Kikuchi, K.; Suzuki, S. *Chem. Lett.* **1985**, 1695. (h) Hori, Y.; Kikuchi, K.; Murata, A.; Suzuki, S. *Chem. Lett.* **1986**, 897. (i) Cook, R. L.; MacDuff, R. C.; Sammells, A. F. *J. Electrochem. Soc.* **1987**, *134*, 2375. (j) Cook, R. L.; MacDuff, R. C.; Sammells, A. F. *J. Electrochem. Soc.* **1988**, *135*, 1320. (k) Kim, J. J.; Summers, D. P.; Frese, K. W. *J. Electroanal. Chem.* **1988**, *245*, 223. (l) Mahmood, M. N.; Masheder, D.; Harty, C. J. *J. Appl. Electrochem.* **1987**, *17*, 1159. (m) Eggins, B. R.; Brown, E. M.; McNeill, E. A.; Grimshaw, J. J. *Tetrahedron Lett.* **1988**, *29*, 945. (n) Eggins, B. R.; Irvine, J. T. S.; Grimshaw, J. *J. Electroanal. Chem.* **1989**, *266*, 125.

0002-7863/91/1513-8455$02.50/0

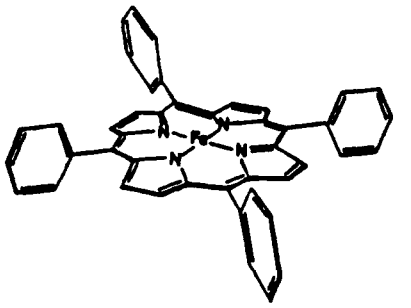

TPP

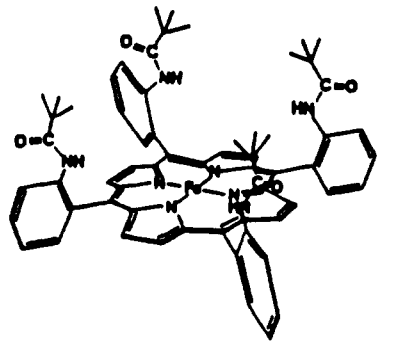

a-PF

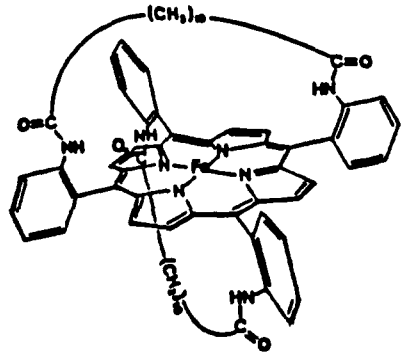

a-(C12)$_2$-CT-TPP

Figure 1. Porphyrins used in this work and their symbolic designations.

catalyst and ceases to act as a simple outer-sphere electron donor. The electrode potential at which the reduction of CO_2 into its radical anion takes place is much more negative than the standard potentials of the reactions leading to the various products evoked earlier. This is one reason that considerable efforts have been made to find catalysts allowing a substantial decrease of these overpotentials. Another motivation has been the search for catalysts able to orient the reaction selectivity toward one of the various above-mentioned products. In this purpose, heterogeneous catalysts, mostly metals, have been used as well as homogeneous molecular catalysts.[7] Concerning the latter, a distinction should

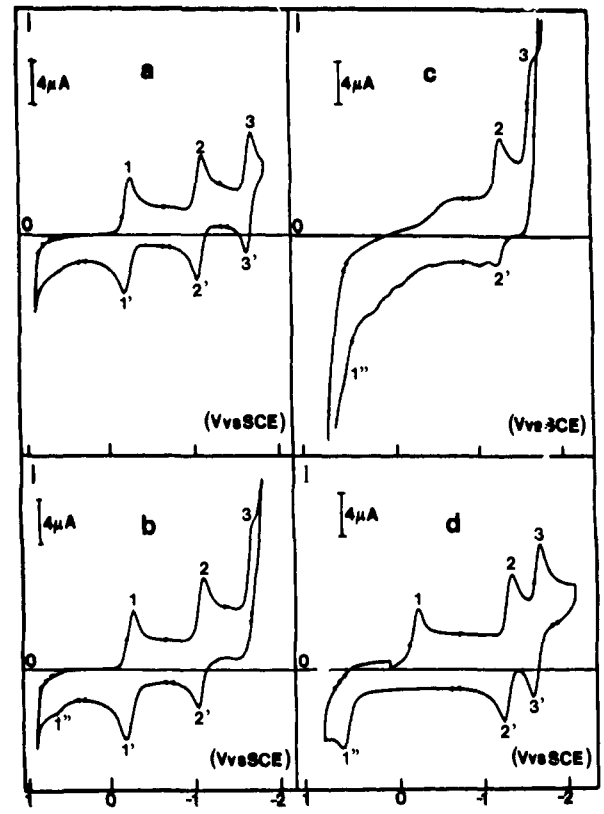

Figure 2. Cyclic voltammetry of TPPFe^{III}Cl (0.5 mM) in DMF + 0.1 M NEt_4ClO_4 on a glassy carbon electrode at 20 °C: (a) alone, (b) under 1 atm of CO_2, (c) under 1 atm of CO_2 with an anodic potential scanning starting beyond the wave where the Fe("0")$^{2-}$ complex is formed, and (d) under 1 atm of CO; scan rate, 0.1 V s^{-1}.

be made between redox catalysts and chemical catalysts.[8] Aromatic and heteroaromatic anion radicals often react as outer-sphere electron donors. However in the case of CO_2 reduction, the $CO_2^{\bullet-}$ anion radical couples with the aromatic anion radical leading to a hydrocarboxylation reaction that destroys the catalyst.[9a] It appears however that benzonitrile,[9b] benzoic esters, and their substituted analogues as well as phthalic esters[2e] escape this rule and are thus able to act as redox catalyst precursors. Oxalate is then the main reaction product[2e,9b] as in the direct reduction of CO_2 on inert electrodes.

Reduced states of transition-metal complexes have been extensively tried as homogeneous catalysts for the electrochemical reduction of CO_2. When catalysis is observed, it is presumably of the chemical type.[8] Interactions between the catalyst and the substrate then exist that are stronger than those involved in a simple outer-sphere electron transfer. One possibility is that the

(6) (a) Vassiliev, Yu. B.; Bagotskii, V. S.; Osetrova, N. V.; Khazova, O. A.; Mayorova, N. A. *J. Electroanal. Chem.* **1985**, *189*, 271. (b) Vassiliev, Yu. B.; Bagotskii, V. S.; Osetrova, N. V.; Mikhailova, A. A. *J. Electroanal. Chem.* **1985**, *189*, 271.

(7) (a) For recent reviews see refs 7b–d. (b) Silvestri, G. In *Carbon Dioxide as a Source of Carbon*; Aresta, M., Forti, G., Eds.; NATO ASI Series: Ser. C, Reidel: Dordrecht, 1987; p 339. (c) Collin, J. P.; Sauvage, J. P. *Coord. Chem. Rev.* **1989**, *93*, 245. (d) Silvestri, G.; Gambino, S.; Filardo, G. In *Enzymatic and Model Carboxylation and Reduction Reactions for CO_2 Utilization*; NATO ASI Series, Reidel: Dordrecht.

(8) (a) In homogeneous catalysis of an electrochemical reduction reaction, the oxidized form of a reversible couple having a standard potential positive to the direct reduction potential of the substrate is introduced into the solution (and vice versa for an oxidation reaction). When the electrode potential reaches the standard potential of this redox couple, its reduced form reacts with the substrate and regenerates the oxidized form, the reduction of which at the electrode surface opens a new catalytic cycle. In redox catalysis,[8b] the reduced form of the couple, i.e., the catalyst, is merely a simple outer-sphere electron donor that shuttles electrons from the electrode to the substrate. This homogeneous electron transfer is subject to the same Marcus limitations as the outer-sphere electron transfer at the electrode. The very existence of a catalytic effect thus derives from a physical rather than a chemical process, namely the dispersion of the electrons in the same three-dimensional space as the substrate instead of the two-dimensional availability of the electrons at the electrode surface.[2c,d,8b] In chemical catalysis,[8b] the interactions, between the catalyst and the substrate are stronger involving the transient formation of an addition product between the catalyst and either the substrate or a group of atoms initially belonging to the substrate. (b) Andrieux, C. P.; Dumas-Bouchiat, J.-M.; Savéant, J.-M. *J. Electroanal. Chem.* **1978**, *87*, 39.

(9) (a) This may even be an interesting procedure to introduce CO_2 groups into organic molecules.[7b,d] (b) Filardo, G.; Gambino, S.; Silvestri, G.; Gennaro, A.; Vianello, E. *J. Electroanal. Chem.* **1984**, *177*, 303.

catalytic reaction starts with the formation of an adduct between the substrate and the catalyst. Several stable adducts between CO_2 and transition-metal complexes have been described.[10] In catalytic systems, however, the adduct should be less stable in regards to the transformation of the CO_2 molecule introduced in the coordination sphere so as to regenerate rapidly the oxidized form of the catalyst and to start a new catalytic cycle.

Water-soluble porphyrins have been used in a few studies. Among them, only the cobalt(I) complexes exhibit some catalytic activity.[11] In the case of *meso*-tetracarboxyphenylporphyrins, the cyclic voltammograms show a catalytic activity of the cobalt(I) complex, and formic acid is detected after electrolysis.[11a,b] With the tetrakis(*p*-trimethylammoniophenyl)porphyrin complex, CO is obtained with a good faradaic yield.[11c-g] With palladium and silver porphyrins in dichloromethane, oxalate is obtained but demetalation rapidly deactivates the catalyst.[11h,i]

Several nonporphyrinic macrocyclic cobalt(II) and nickel(I) complexes catalyze the reduction of CO_2 in water or in partially aqueous media.[12] A mixture of CO and H_2 is generally obtained, the composition of which depends upon the nature of the complex and the composition of the reaction medium. The best results were obtained with nickel cyclam which led to the selective production of CO with excellent turnovers per hour at −1.3 V vs SCE.[12d-f] The catalytic process is not strictly speaking homogeneous since the reaction appears to take place at the surface of the mercury used as electrode material. Another series of attempts concerns the use of transition-metal complexes with 2,2′-bipyridine or similar molecules as ligands, in dry or aqueous DMF and CH_3CN.[13] The identification of the actual species that acts as catalyst is not an easy task. In the case of $Re^{II}(bpy)(CO)_3Cl$, one of the most efficient system in the series, the catalyst seems to be a Re^0 complex where all the starting ligands are present but the bipyridine is monocoordinated.[13c,g] Other transition-metal complexes have also been investigated, namely complexes bearing phosphine ligands[14] and iron–sulfur clusters,[15] but do not seem very stable on the preparative scale.

Films of metallophthalocyanines deposited onto electrode surfaces have also been used as catalysts for the reduction of CO_2 in water.[16] Other attempts of supported homogeneous catalysis have consisted in incorporating transition-metal complexes catalysts into polymeric structures deposited on the electrode.[17] So far they have not been very successful either because of rapid destruction of the catalyst or because insufficient electron conduction through the polymer coating. Mixed systems, in which homogeneous catalysts are associated with electrode coatings (for example the Prussian blue/Everit salt couple), have been shown to produce methanol when the solvent is itself methanol or another primary alcohol.[18] Good faradaic yields could then be obtained at rather positive potential, but the turnovers per hour remain quite low.

Previous work has shown that iron("0") porphyrins do not simply react as outer-sphere electron donors in spite of the fact that they form with the corresponding iron(I) complex a fast and perfectly reversible redox couple.[19] For example, their reaction

(10) (a) Bristow, G. S.; Hitchcock, P. B.; Lappert, M. F. *J. Chem. Soc., Chem. Commun.* **1981**, 1145. (b) Gambarotta, S.; Floriani, C.; Chiesi-Villa, A.; Guastini, C. *J. Am. Chem. Soc.* **1985**, *107*, 2985. (c) Alvarez, R.; Carmona, E.; Guttierrez-Puebla, E.; Marin, J. M.; Monge, A.; Poveda, M. L. *J. Chem. Soc., Chem. Commun.* **1984**, *924*, 1326. (d) Alvarez, R.; Carmona, E.; Marin, J. M.; Poveda, M. L.; Guttierrez-Puebla, E.; Monge, A. *J. Am. Chem. Soc.* **1986**, 2286. (e) Calabrese, J. C.; Herskovitz, T.; Kinney, J. B. *J. Am. Chem. Soc.* **1983**, *105*, 5914. (f) Herskovitz, T. *Inorg. Synth.* **1982**, *21*, 99. (g) Herskovitz, T.; Guggenberger, L. J. *J. Am. Chem. Soc.* **1976**, *98*, 1615. (h) Aresta, M.; Nobile, C. F.; Albano, V. G.; Forni, E.; Manassero, M. *J. Chem. Soc., Chem. Commun.* **1975**, 636. (i) Braunstein, P.; Matt, D.; Nobel, D. *J. Am. Chem. Soc.* **1988**, *110*, 3207. (j) Beck, W.; Raab, K.; Nagel, U.; Steimann, M. *Angew. Chem., Int. Ed. Engl.* **1982**, *21*, 526. (k) Lundquist, E. G.; Huffman, J. C.; Caulton, K. G. *J. Am. Chem. Soc.* **1986**, *108*, 8309. (l) Audett, J. D.; Collins, T. J.; Santarsiero, B. D.; Spies, G. H. *J. Am. Chem. Soc.* **1982**, *104*, 7352. (m) Eady, C. R.; Guy, J. J.; Johnson, B. F. G.; Lewis, J.; Malatesta, M. C.; Sheldrick, G. M. *J. Chem. Soc., Chem. Commun.* **1976**, 602. (n) Guy, J. J.; Sheldrick, G. M. *Acta Crystallogr. Sect. B* **1978**, *34*, 1718. (o) Fachinetti, G.; Floriani, C. *J. Chem. Soc., Chem. Commun.* **1974**, 615. (p) Fachinetti, G.; Floriani, C.; Zanazzi, P. F. *J. Am. Chem. Soc.* **1978**, *100*, 7405. (q) Fachinetti, G.; Floriani, C.; Zanazzi, P. F.; Zanzari, A. R. *Inorg. Chem.* **1978**, *18*, 3469. (r) Gambarotta, S.; Arena, F.; Floriani, C.; Zanazzi, P. F. *J. Am. Chem. Soc.* **1982**, *104*, 5082. (s) Floriani, C. *Pure Appl. Chem.* **1983**, *55*, 1. (t) Of particular interest for the present discussion is the case of Co(I) salen complexes in which the formation of a stable CO_2 adduct is favored by alkali cations.[10o-t]

(11) (a) Hiratsuka, H.; Takahashi, K.; Sasaki, H.; Toshima, S. *Chem. Lett.* **1977**, 1137. (b) Takahashi, K.; Hiratsuka, K.; Sasaki, H.; Toshima, S. *Chem. Lett.* **1979**, 305. (c) Cao, X.; Huang, C.; Wang, M. *Gaodeng Xuexiao Huaxue Xuebao* **1983**, *4*, 549; *Chem. Abstr. 100*, 058659. (d) Cao, X.; Mu, Y.; Wang, M.; Luan, L. *Huaxue Xuebao* **1986**, *44*, 220; *Chem. Abstr. 104*, 195348. (e) Cao, X.; Mu, Y.; Wang, M.; Huang, C. *Gaodeng Xuexiao Huaxue Xuebao* **1986**, *7*, 302; *Chem. Abstr. 106*, 074777. (f) Cao, X.; Zheng, G. *Gaodeng Xuexiao Huaxue Xuebao* **1987**, *8*, 686; *Chem. Abstr. 108*, 194575. (g) Cao, X.; Zheng, G.; Teng, Y. *Gaodeng Xuexiao Huaxue Xuebao* **1988**, *9*, 861; *Chem. Abstr. 110*, 30379. (h) Becker, J. Y.; Vainas, B.; Eger, R.; Kaufman, L. *J. Chem. Soc., Chem. Commun.* **1985**, 1471. (i) Catalysis may be in this case of the redox type rather than of the chemical type which would fall in line with an anion radical character of the reduced state of the Pd(II) and Ag(II) porphyrins rather than a Pd(I) and Ag(I) character.

(12) (a) Fischer, B.; Eisenberg, R. *J. Am. Chem. Soc.* **1980**, *102*, 7361–7363. (b) Tinnemans, A. H. A.; Koster, T. P. M.; Thewissen, D. H. M. W.; Mackor, A. M. *Recl. Trav. Chim. Pays-Bas* **1984**, *103*, 288. (c) Pearce, D. J.; Pletcher, D. *J. Electroanal. Chem.* **1986**, *197*, 317. (d) Beley, M.; Collin, J. P.; Ruppert, R.; Sauvage, J. P. *J. Chem. Soc., Chem. Commun.* **1984**, 1315. (e) Beley, M.; Collin, J. P.; Ruppert, R.; Sauvage, J. P. *J. Am. Chem. Soc.* **1986**, *108*, 7461. (f) Collin, J. P.; Jouaiti, A.; Sauvage, J. P. *Inorg. Chem.* **1988**, *27*, 1986. (g) Fujihira, M.; Hirata, Y.; Suga, K. *J. Electroanal. Chem.* **1990**, *292*, 199.

(13) (a) Daniele, S.; Ugo, P.; Bontempelli, G.; Fiorani, M. *J. Electroanal. Chem.* **1987**, *219*, 259. (b) Hawecker, J.; Lehn, J. M.; Ziessel, R. *J. Chem. Soc., Chem. Commun.* **1984**, 328. (c) Hawecker, J.; Lehn, J. M.; Ziessel, R. *Helv. Chim. Acta* **1986**, *69*, 1990. (d) Sullivan, B. P.; Meyer, T. J. *J. Chem. Soc., Chem. Commun.* **1984**, 1244. (e) Sullivan, B. P.; Bolinger, C. M.; Conrad, D.; Vining, W. J.; Meyer, T. J. *J. Chem. Soc., Chem. Commun.* **1985**, 1414. (f) Sullivan, B. P.; Meyer, T. J. *Organometallics* **1986**, *5*, 1500. (g) Breikss, A. I.; Abruña, H. D. *J. Electroanal. Chem.* **1986**, *201*, 347. (h) Bruce, M. R. M.; Megehee, E.; Sullivan, B. P.; Thorp, H. R.; O'Toole, T.; Downard, A.; Meyer, T. J. *Organometallics* **1988**, *7*, 238. (i) Bolinger, C. M.; Story, N.; Sullivan, B. P.; Meyer, T. J. *Inorg. Chem.* **1988**, *27*, 4582. (j) Bolinger, C. M.; Sullivan, B. P.; Conrad, D.; Gilbert, J. A.; Story, N.; Meyer, T. J. *J. Chem. Soc., Chem. Commun.* **1985**, 796. (k) Ishida, H.; Tanaka, K.; Tanaka, T. *Chem. Lett.* **1985**, 405. (l) Ishida, H.; Tanaka, H.; Tanaka, K.; Tanaka, T. *J. Chem. Soc., Chem. Commun.* **1987**, 131. (m) Ishida, H.; Tanaka, K.; Tanaka, T. *Organometallics* **1987**, *6*, 181. (n) Ishida, H.; Tanaka, H.; Tanaka, K.; Tanaka, T. *Chem. Lett.* **1987**, 597. (o) Tanaka, K.; Miyamoto, H.; Tanaka, T. *Chem. Lett.* **1988**, 2033. (p) Garnier, L.; Rollin, Y.; Pĕrichon, J. *New J. Chem.* **1989**, *13*, 53.

(14) (a) Slater, S.; Wagenknecht, J. H. *J. Am. Chem. Soc.* **1984**, *106*, 5367. (b) Dubois, D. L.; Miedaner, A. *J. Am. Chem. Soc.* **1987**, *109*, 113.

(15) (a) Matsumoto, Y.; Uchida, Y.; Hidai, M.; Tesuka, M.; Yajima, T.; Tsuchiya, A. *J. Am. Chem. Soc.* **1982**, *104*, 6834. (b) Nakazawa, M.; Mizobe, Y.; Matsumoto, Y.; Uchida, Y.; Tesuka, M.; Hidai, M. *Bull. Chem. Soc. Jpn.* **1986**, *59*, 809.

(16) (a) With CO and Ni as the central metal,[11a,16b-g] high yields of CO are obtained although another study indicates that formic acid is the main reduction product.[16h] With Sn, Pb, and In, the main products are formic acid and hydrogen.[16g] With Cu, Ga, Ti, the main products are CO and H_2 but also methane with a respectable yield (up to 30%),[16g] whereas with Fe, Zn, and Pd, CO is obtained but with a lower yield than with CO and Ni. Hydrogen is solely obtained with Mg, V, Mn, Pt, and with the free base. (b) Meshitsuka, S.; Ichikawa, M.; Tamaru, K. *J. Chem. Soc., Chem. Commun.* **1974**, 158. (c) Lieber, M. C.; Lewis, N. S. *J. Am. Chem. Soc.* **1984**, *106*, 5033. (d) Mahmood, M. N.; Masheder, D.; Harty, C. J. *J. Appl. Electrochem.* **1987**, *17*, 1159. (e) Mahmood, M. N.; Masheder, D.; Harty, C. J. *J. Appl. Electrochem.* **1987**, *17*, 1223. (f) Tanabe, H.; Ohno, K. *Electrochim. Acta* **1987**, *32*, 1121. (g) Furuya, N.; Matsui, K. *J. Electroanal. Chem.* **1989**, *271*, 181. (h) Kapusta, S.; Hackerman, N. *J. Electrochem. Soc.* **1984**, *131*, 1511.

(17) (a) O'Toole, T. R.; Margerum, L. D.; Westmoreland, T. D.; Vining, W. J.; Murray, R. W.; Meyer, T. J. *J. Chem. Soc., Chem. Commun.* **1985**, 1416. (b) Cabrera, C. R.; Abruna, H. D. *J. Electroanal. Chem.* **1986**, *209*, 101. (c) Cosnier, S.; Deronzier, A.; Moutet, J. C. *J. Electroanal. Chem.* **1986**, *207*, 315.

(18) (a) Ogura, K.; Takamagari, K. *J. Chem. Soc., Dalton Trans.* **1986**, 1519. (b) Ogura, K.; Takagi, M. *J. Electroanal. Chem.* **1986**, *206*, 209. (c) Ogura, K.; Yoshida, I. *J. Mol. Catal.* **1986**, *34*, 67. (d) Ogura, K.; Fujita, M. *J. Mol. Catal.* **1987**, *41*, 303. (e) Ogura, K.; Yoshida, I. *Electrochim. Acta.* **1987**, *32*, 1191. (f) Ogura, K. *J. Electrochem. Soc.* **1987**, *134*, 2749. (g) Ogura, K.; Uchida, H. *J. Electroanal. Chem.* **1987**, *220*, 333. (h) Ogura, K.; Yoshida, I. *J. Mol. Catal.* **1988**, *47*, 51.

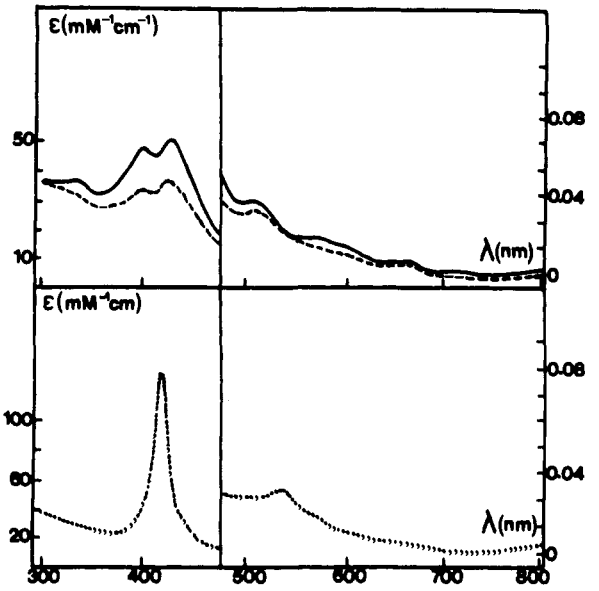

Figure 3. Thin-layer UV-vis spectroelectrochemistry of TPPFeCl (0.1 mM) in DMF + 0.1 M NEt_4ClO_4 under 1 atm of CO_2: (—) electrolysis at −1.2 V vs SCE (formation of the iron(I) porphyrin), (--) electrolysis at −1.8 V vs SCE (beyond the catalytic wave), and (···) reoxidation at −1.6 V vs SCE (formation of $Fe^{II}CO$).

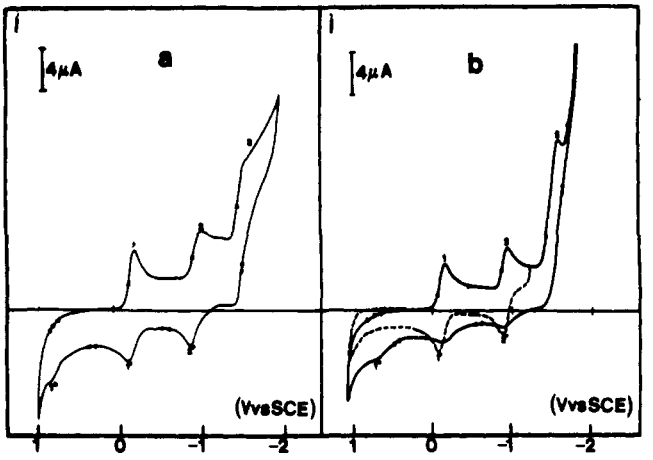

Figure 4. Cyclic voltammetry of a-PF-FeCl (a) and a-$(C12)_2$-CTTPPFeCl and (b) in DMF + 0.1 M NEt_4ClO_4 at 20 °C on a glassy carbon electrode under 1 atm of CO_2; porphyrin concentration, 0.5 mM; scan rate, 0.1 $V·s^{-1}$.

with aliphatic monohalides involves the iron atom rather than the porphyrin ring, giving rise to the corresponding σ-alkyliron(II) complexes.[19a-c] In the absence of steric constraints, they react much faster than typical outer-sphere electron donors such as aromatic anion radicals, pointing to the existence of bonded iron–carbon interactions in the transition state.[19b] Similarly, the reaction of iron("0") porphyrins with vicinal dibromides, leading to the corresponding olefins, involves the iron atom and proceeds in an inner-sphere manner (Br^+ abstraction concerted with the elimination of the other bromine atom under the form of Br^-).[19d,e] These results show that iron("0") porphyrins are able to develop an iron-centered chemistry involving bonded interactions and eventually bond formation with electrophilic centers. There is thus some hope that iron("0") porphyrins may serve as chemical catalysts of the electrochemical reduction of carbon dioxide. It is however not excluded that CO_2 may bind to the porphyrin ring rather than, or in competition with, a reaction taking place in the coordination sphere of the iron atom.[20] Preliminary cyclic voltammetric experiments have shown that a catalytic current is observed at the level of the $Fe(I)^-/Fe("0")^{2-}$ wave when CO_2 is present in the solution.[21] The purpose of the work described in the following was to carry out a more complete investigation of the problem both in terms of preparative scale electrolysis and mechanism analysis. It will be seen that the addition of magnesium ions to the solution allows a spectacular improvement of the catalytic efficiency as well as of the stability of the catalyst.

Results and Discussion

The porphyrins we investigated are shown, together with their symbolic designation, in Figure 1. Besides the classical TPP, we used a basket-handle and a picket-fence porphyrin containing in their superstructures secondary amide groups in close vicinity to the porphyrin ring. In all cases, the starting complex was the iron(III) porphyrin chloride.

Preliminary Cyclic Voltammetric and Spectroelectrochemical Investigations. In the absence of iron porphyrin, the cyclic voltammogram of a DMF solution (+0.1 M NEt_4ClO_4) at 20 °C on a glassy carbon electrode under 1 atm of CO_2 (i.e., a concentration of 0.235 M[22]) shows a steep rise of the current at −2.1 V vs SCE (instead of −2.7 V vs SCE in the absence of CO_2) due to the reduction of CO_2 at the electrode. Typical experiments showing the effect of CO_2 on the cyclic voltammetry of the $TPPFe^{III}Cl$ porphyrin are summarized in Figure 2. The porphyrin alone exhibits three reversible waves corresponding to the following redox couples $Fe(III)^+/Fe(II)$ (1/1′), $Fe(II)/Fe(I)^-$ (2/2′), and $Fe(I)^-/Fe("0")^{2-}$ (3/3′). Under 1 atm of CO_2, wave 3 increases in height and becomes irreversible. At the same time a new wave, denoted 1″, appears on the anodic scan. The appearance of this new wave points to the formation of CO as a result of the catalytic increase of wave 3. Indeed, as can be seen in Figure 2d, one effect of CO on the cyclic voltammetry of the porphyrin is to make wave 1′ disappear at the expense of wave 1″. Wave 1 remains practically unaffected, the reversible wave 2/2′ shifts cathodically, and the reversible wave 3/3′ remains practically the same. These effects are essentially a reflection of the strong complexation of the iron(II) porphyrin by CO. In contrast, the iron(III) porphyrin does not bind CO,[23] and the iron(I) porphyrin binds CO to a much

(19) (a) Lexa, D.; Savéant, J.-M.; Wang, D. L. *Organometallics* **1986**, *5*, 1428. (b) Lexa, D.; Savéant, J.-M.; Su, K. B.; Wang, D. L. *J. Am. Chem. Soc.* **1988**, *110*, 7617. (c) Gueutin, C.; Lexa, D.; Savéant, J.-M.; Wang, D. L. *Organometallics* **1989**, *8*, 1607. (d) Lexa, D.; Savéant, J.-M.; Su, K. B.; Wang, D. L. *J. Am. Chem. Soc.* **1987**, *109*, 6464. (e) Lexa, D.; Savéant, J.-M.; Schäfer, H. J.; Su, K. B.; Vering, B.; Wang, D. L. *J. Am. Chem. Soc.* **1990**, *112*, 6162.

(20) (a) The question of the respective weights of iron(0) and iron(I) anion radical resonant forms in the electronic description of iron("0") porphyrins is not completely settled for the moment. With superstructured porphyrins bearing secondary amide groups such as those shown in Figure 1, one readily obtains the reversible formation of the iron("0") complex in thin-layer spectroelectrochemistry with DMF as the solvent and 0.1 M NEt_4ClO_4 as supporting electrolyte.[20b] With TPP (Figure 1), reversibility is only partial, and a spectrum reminiscent of a σ-alkyliron(II) porphyrins[19a-c] appears superimposed with the same spectrum as that obtained with the superstructured porphyrins. Repeated recrystallization of the supporting electrolyte makes the second spectrum increase at the expense of the first. The spectrum thus assigned to the iron("0") porphyrins in DMF in the presence of NEt_4^+ cations is of the hyperporphyrins type and is clearly different from that reported for the same complex obtained from the reaction with a sodium mirror in THF.[20c,d] The description of the latter complex as a structure where the main resonant forms would be an iron(I) anion radical[20d,e] and an iron(II) dianion[20e] is therefore not suited to the complex we obtain in DMF with NEt_4^+ as countercation. The latter seems to have more electronic density on the iron center although it is not excluded that some electron density may remain on the ring. (b) Hammouche, M.; Lexa, D.; Savéant, J.-M., unpublished results. (c) Hickman, D. L.; Shiragi, A.; Goff, H. M. *Inorg. Chem.* **1985**, *24*, 563. (d) Mashiko, T.; Reed, C. A.; Haller, K. J.; Scheidt, W. R. *Inorg. Chem.* **1984**, *23*, 3192. (e) Teraoka, J.; Hashimoto, S.; Sugimoto, H.; Mori, M.; Kitagawa, T. *J. Am. Chem. Soc.* **1987**, *109*, 180.

(21) Hammouche, M.; Lexa, D.; Savéant, J.-M.; Momenteau, M. *J. Electroanal.* **1988**, *249*, 347.

(22) Gennaro, A.; Isse, A. A.; Vianello, E. *J. Electroanal. Chem.* **1990**, *289*, 203.

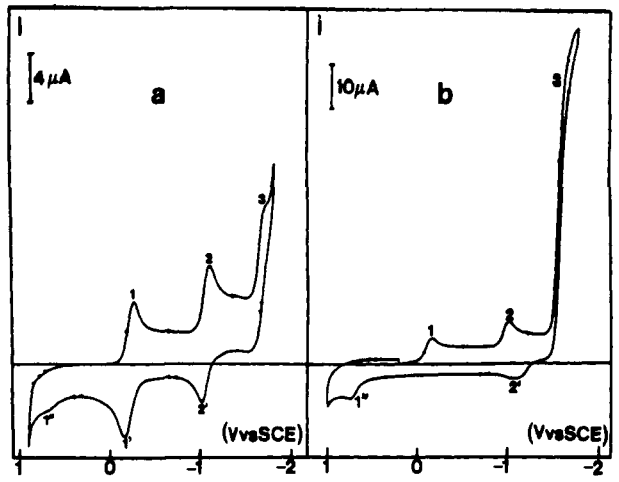

Figure 5. Cyclic voltammetry of TPPFeCl (0.5 mM) in DMF + 0.1 M NEt_4ClO_4 under 1 atm of CO_2 in the absence (a) and in the presence (b) of Mg^{2+} ions (23 mM dry $Mg(ClO_4)_2$): temperature, 20 °C; scan rate, 0.1 $V \cdot s^{-1}$; working electrode, glassy carbon.

lesser extent than does the iron(II) porphyrin.[2] The fact that both waves 1′ and 1″ are present on the anodic scan shows that the concentration of CO formed at the level of wave 3 is significantly less than the concentration corresponding to 1 atm (2.7 mM at 20 °C[24]). The amount of CO formed is not however simply proportional to the ratio between wave 1″ and the sum of waves 1′ + 1″, since the oxidation at the level of wave 1′ occurs along a "CE" mechanism[2c]:

$$Fe^{II}CO \rightleftarrows Fe(II) + CO$$

$$Fe(II) - e^- \rightleftarrows Fe(III)^+$$

Wave 1″ thus corresponds to the fraction of $Fe^{II}CO$ that has not been oxidized through its decomposition into Fe(II) and CO for kinetic reasons.

The decrease of wave 1′ at the expense of wave 1″ appears even more clearly when the potential is scanned anodically after setting the initial potential beyond wave 3, i.e., at a potential where the catalytic reaction takes place. We also note a modification of wave 1 which is consistent with the concomitant formation of carbonate ions that would complex the iron(III) porphyrin competitively with the chloride ions.[23f] It is also noted that wave 2′ decreases and that other small waves appear on the anodic scan indicating that a fraction of the porphyrin has been transformed during the catalytic process.

These findings are confirmed by thin-layer spectroelectrochemistry (Figure 3). The formation of CO at the catalytic wave is seen upon reoxidation at the potential where iron(I) is oxidized into iron(II) which then appears as its CO complex as checked by comparison with an authentic sample obtained from the electrolysis of Fe(III) to Fe(II) under 1 atm of CO. We again note, at this level the disappearance of a small fraction (ca. 20%) of the porphyrin during the catalytic process.

Similar results were obtained both in cyclic voltammetry (Figure 4) and in thin-layer spectroelectrochemistry with the two superstructured porphyrins shown in Figure 1. The catalytic wave

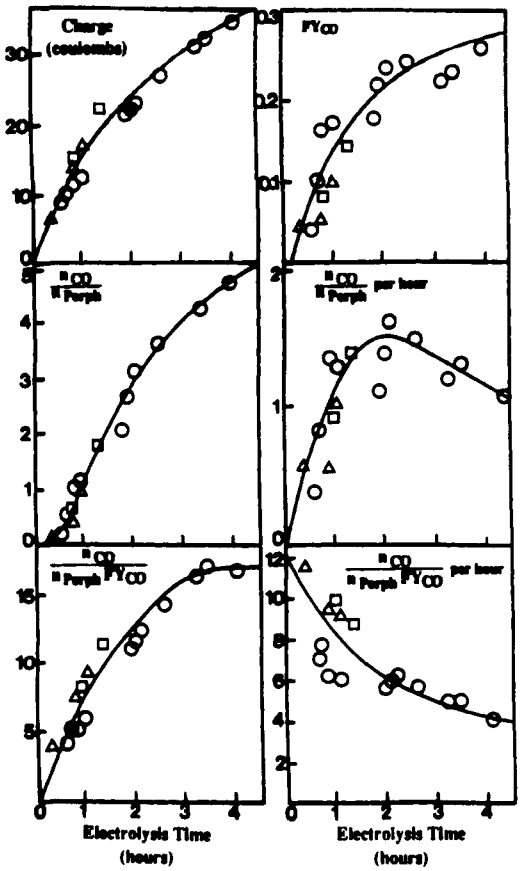

Figure 6. Electrolysis of CO_2 (1 atm) in the presence of $TPPFe^I$ (0.5 mM) in DMF + 0.1 M NEt_4ClO_4 on a mercury pool electrode in a two-compartment cell: charge, faradaic yield in CO (FY_{CO}), turnover number, (n_{CO}/n_{porph}) turnover number per hour; turnover number for the production of CO ($n_{CO}/n_{porph}FY_{CO}$), turnover number for the production of CO per hour as functions of the electrolysis time. Electrolysis potential: −1.8 V vs SCE: temperature, 20 °C. The three types of points (△, □, ○) correspond to three different runs.

is higher, and the production of CO is larger than in the case of TPP.

Addition of magnesium cations to the solution in the form of nonhydrated $Mg(ClO_4)_2$ spectacularly enhances the catalytic wave and the production of CO as can be seen in Figure 5 in the case of TPP. Wave 1′ completely disappears at the expense of wave 1″ and a substantial portion of wave 2′ represents the direct oxidation of the Fe^ICO^- complex along a "CE" mechanism:

$$Fe(I)^- + CO \rightleftarrows Fe^{II}CO^-$$

$$Fe^ICO^- - e \rightleftarrows Fe^{II}CO$$

Similar observations were made with the two superstructured porphyrins. Sodium ions, introduced into the solution in the form of $NaAsF_6$ also produces the same effect although it is weaker than that of Mg^{2+} ions for the same concentration. Addition of LiCl, $BaCl_2$, or $AlCl_3$ results also in an enhancement of the catalytic wave and of the production of CO. However much larger concentrations than with $Mg(ClO_4)_2$ are required to obtain a similar effect.

As described above, the cyclic voltammetric investigations were carried out on glassy carbon disk electrodes. Preliminary experiments carried out with a carbon crucible as working electrode showed that this material is not suitable for preparative scale electrolyses in the sense that the electrode is rapidly passivated. Satisfactory results were obtained with a mercury pool electrode stirred with a magnetic stirrer. For this reason we examined, through a series of test experiments, whether or not the cyclic voltammetric results are affected by the change of the working electrode from a glassy carbon disk to a mercury drop hung onto a gold disk. In the absence of porphyrins the current rise due to the direct reduction of CO_2 under 1 atm shifts negatively by about

(23) (a) The iron(III) porphyrin has no affinity for CO but has a good affinity for Cl^-. In the presence of CO as well as in its absence, wave 1 represents the reduction of $Fe^{III}Cl$ into $Fe^{II}Cl^-$.[23b,e] The fact that wave 1 is insensitive to the presence of CO indicates that CO binds to the iron(II) porphyrin after irreversible expulsion of the Cl^- ligand: $Fe^{III}Cl + e^- \rightleftarrows Fe^{II}Cl^-$, $Fe^{II}Cl^- \rightarrow Fe^-(II) + Cl^-$, $Fe(II) + CO \rightarrow Fe^{II}CO$ (the binding of Fe(II) with CO is faster than its binding with Cl^-). (b) Lexa, D.; Momenteau, M.; Rentien, P.; Rytz, G.; Savéant, J.-M.; Xu, F. *J. Am. Chem. Soc.* **1984**, *106*, 4765. (c) Lexa, D.; Rentien, P.; Xu, F. *J. Electroanal. Chem.* **1985**, *191*, 253. (d) Savéant, J.-M.; Xu, F. *J. Electroanal. Chem.* **1986**, *208*, 197. (e) Gueutin, C.; Lexa, D.; Momenteau, M.; Savéant, J. M.; Xu, F. *Inorg. Chem.* **1986**, *25*, 4294. (f) This was confirmed by the cyclic voltammetry of $TPPFe^{III}Cl$ in the presence of $CO_3(NEt_4)_2$.

(24) Taqui Khan, M. M.; Halligudi, S. B.; Shukia, S. *J. Chem. Eng. Data* **1989**, *34*, 353.

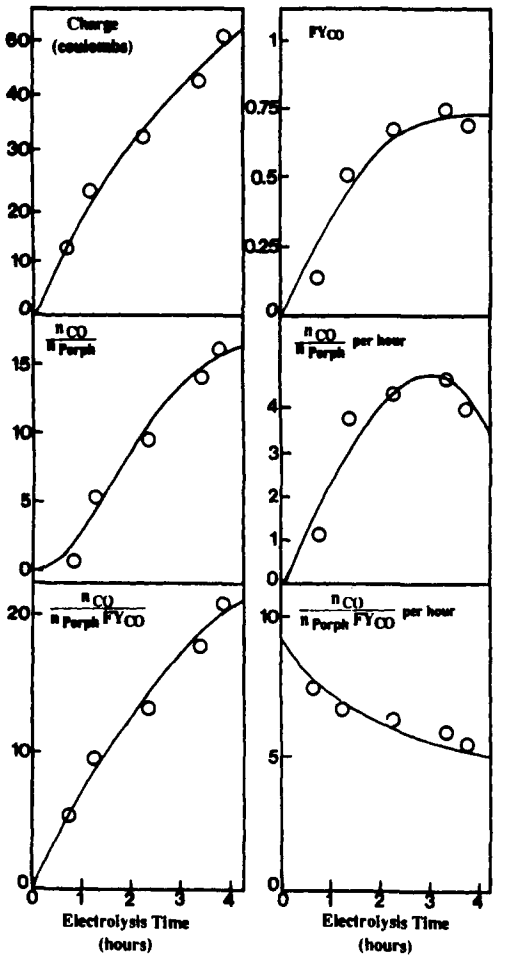

Figure 7. Electrolysis of CO_2 in the presence of a-$(C12)_2$-CT-TPPFe^I in DMF + 0.1 M NEt_4ClO_4 on a mercury pool electrode in a two-compartment cell: charge, faradaic yield in CO(FY_{CO}), turnover number (n_{CO}/n_{porph}), turnover number per hour, turnover number for the production of CO ($n_{CO}/n_{porph}FY_{CO}$), turnover number for the production of CO per hour as functions of the electrolysis time: electrolysis potential, -1.8 V vs SCE; temperature, 20 °C.

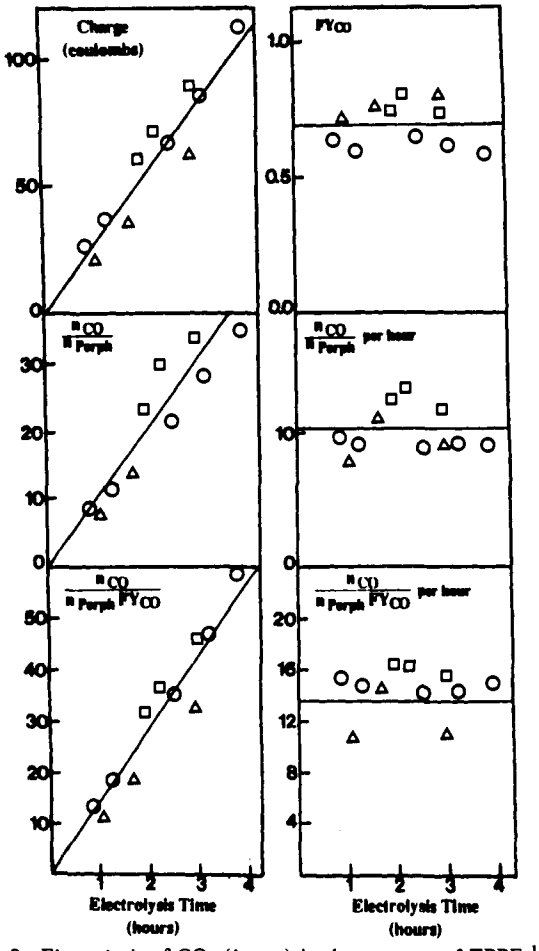

Figure 8. Electrolysis of CO_2 (1 atm) in the presence of TPPFe^I (0.5 mM) and Mg^{2+} ions (24 mM) in DMF + 0.1 M NEt_4ClO_4 on a mercury pool electrode in an undivided cell with a soluble magnesium anode: charge, faradaic yield in CO (FY_{CO}), turnover number (n_{CO}/n_{porph}), turnover number per hour, turnover number for the production of CO ($n_{CO}/n_{porph}FY_{CO}$), turnover number for the production of CO per hour as functions of the electrolysis time: electrolysis potential, -1.7 V vs SCE; temperature, 20 °C. The three types of points (△, □, ○) correspond to three different runs.

200 mV from the first to the second electrode, but the waves of the porphyrins in the absence and in the presence of CO_2 (with or without Mg^{2+} ions) showed no significant variations.

Preparative-Scale Electrolyses. The electrolyses were carried out in a gas-tight cell containing 75 cm^3 of CO_2 at atmospheric pressure in the gas phase with a volume of solution of 20 cm^3 and a mercury pool electrode of 10 cm^2. Two types of anodes were used. In the first set of experiments, we used a platinum wire anode separated from the cathodic compartment by a Nafion membrane, whereas in the second series of experiments, a magnesium anode was used with no separation from the cathodic compartment.[25] Figure 6 summarizes the results obtained with the iron tetraphenyl porphyrins in terms of charge passed, faradaic yield in CO (based on the consumption of two electrons per molecule of CO formed), turnover numbers and turnover numbers per hour, as functions of time. CO was formed in all cases, whereas no significant amounts of formaldehyde, formate, or hydrogen were detected. The faradaic yields for the formation of CO and the time-dependent turnover numbers decreased with time pointing to a rapid destruction of the catalyst. This was also indicated by the change in color of the solution, which passed from reddish-brown to green. Cyclic voltammetry and UV–vis spectrometry of the solution at the end of the electrolysis confirmed the destruction of the porphyrin. The cyclic voltammogram and UV–vis spectrum then obtained are very similar to those obtained in the same type of electrolysis carried out with TPPZn at the potential of its second reversible reduction wave, i.e., at the potential of the $TPPZn^{II\bullet-}/TPPZn^{II2-}$ redox couple. The UV–vis spectra thus obtained indicate that the porphyrin ring has undergone partial saturation by reference to the results previously obtained in the electrochemical reduction of TPPZn.[26] The ring saturation may be caused by carboxylation or alternatively by protonation since the presence of CO_2 renders the residual water in DMF more acidic. Figure 7 summarizes the same type of results obtained with the iron a-$(C12)_2$-CT-TPP instead of the iron TPP. There is an improvement of the faradaic yield in CO, but the porphyrin still disappears with time.

In the second series of experiments not only a one-compartment cell with a soluble magnesium anode was used but also nonhydrated magnesium perchlorate was added to the solution. We noted that the mere use of the magnesium anode did not bring about the improvements in CO yield and stability of the catalyst observed when $Mg(ClO_4)_2$ is introduced in the solution from the start of the electrolysis. This is presumably due to the fact that not enough Mg^{2+} ions produced at the anode have reached the vicinity of the cathode to prevent the destruction of the catalyst in the beginning of the electrolysis. Typical results obtained with TPPFe^I in the presence of Mg^{2+} are summarized in Figure 8. The

(25) (a) Silvestri, G.; Gambino, S.; Filardo, G.; Guainazzi, M.; Ercoli, R. *Gazz. Chim. Ital.* **1972**, *102*, 818. (b) Sibille, S.; Coulombeix, J.; Perichon, J.; Fuch, J. M.; Mortreux, A.; Petit, F. *J. Mol. Catal.* **1985**, *32*, 239. (c) Chaussard, J.; Folest, J. C.; Nédélec, J. Y.; Périchon, J.; Sibille, S.; Troupel, M. *Synthesis* **1990**, 369.

(26) Lanese, J. G.; Wilson, G. S. *J. Electrochem. Soc.* **1972**, *119*, 8, 1039.

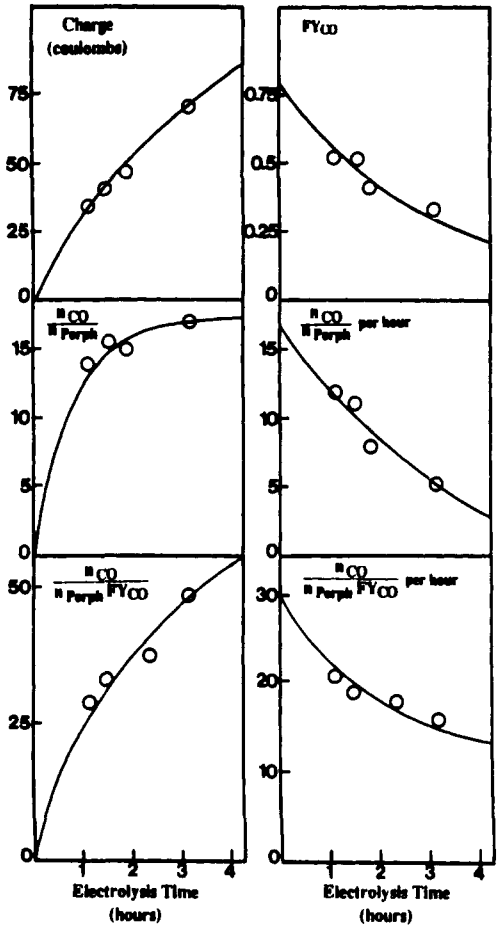

Figure 9. Electrolysis of CO_2 (1 atm) in the presence of a-$(C12)_2$-CT-TPPFe[1] (0.5 mM) and Mg^{2+} ions (15 mM) in DMF + 0.1 M NEt_4ClO_4 on a mercury pool electrode in undivided cell with a soluble magnesium anode: charge, faradaic yield in CO (FY_{CO}), turnover number (n_{CO}/n_{porph}), turnover number per hour, turnover number for the production of CO ($n_{CO}/n_{porph}FY_{CO}$), turnover number for the production of CO per hour as functions of the electrolysis time: electrolysis potential, −1.7 V vs SCE; temperature, 20 °C.

faradaic yields are much larger than in the absence of Mg^{2+} ions and about constant in time (70% in average). After 4 h of electrolysis, there is no appreciable degradation of the porphyrin as confirmed by cyclic voltammetric and UV–vis spectrometric analysis of the solution.

With the a-$(C12)_2$-CT-TPP porphyrins (Figure 9) the introduction of $Mg(ClO_4)_2$ into the solution also brought about some improvement but much less than in the case of TPP. In particular, the degradation of the porphyrin could not be avoided.

The best catalytic system thus consists of the simple iron TPP associated with Mg^{2+} ions. It compares with other homogeneous systems in similar solvents. For example, the turnover number per hour is about ten times that of $Re(bpy)(CO)_3Cl$.[13b] The electrolysis potential is however ca. 200 mV more negative in our case than in the $Re(bpy)(CO)_3Cl$[13b] case.

Analysis of the Mechanism of the Catalytic Reaction. With all the porphyrins, the catalytic wave increases substantially upon decreasing the temperature both in the absence and presence of Mg^{2+} ions. This is illustrated in Figure 10 with the example of TPP. The increase of the catalytic current is essentially a reflection of the increase of the CO_2 concentration as the temperature is lowered. The CO_2 concentration in DMF is 0.23 M at 20 °C and 1.33 M at −40 °C.[22] It is remarkable that this factor is not compensated by a decrease of the rate-determining kinetic constant of the reaction. It also appears that, at −40 °C, the porphyrin is not appreciably destroyed within the time scale of slow scan cyclic voltammetry even in the absence of Mg^{2+} cations. This allowed us to undertake a mechanistic analysis of the catalytic process at −40 °C in the presence and in the absence of Mg^{2+} ions,

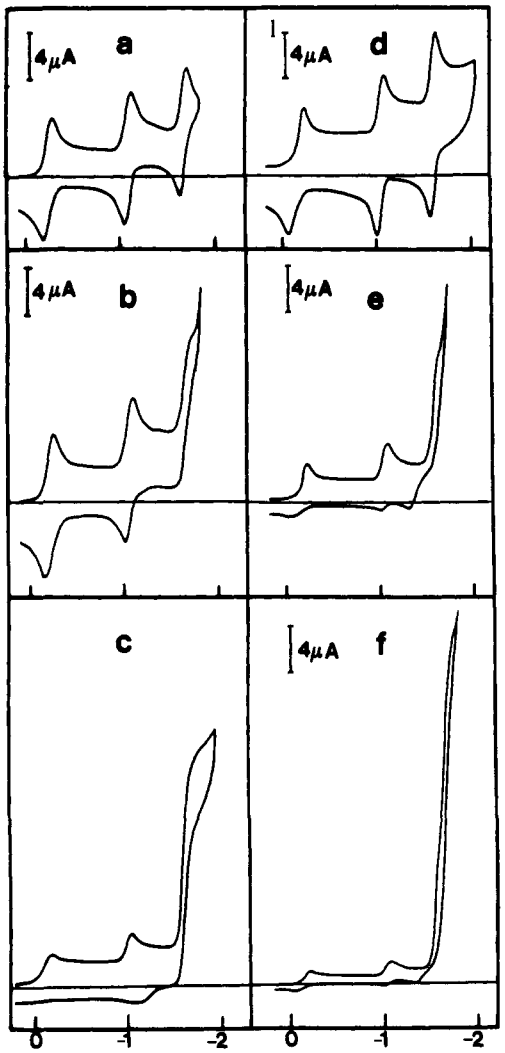

Figure 10. Effect of temperature on the catalysis of the reduction of CO_2 by the TPPFe("0")$^{2-}$ porphyrins. Cyclic voltammetry of TPPFeCl (0.5 mM) in DMF + 0.1 M NEt_4ClO_4 on a glassy carbon electrode is represented: scan rate, 0.1 $V{\cdot}s^{-1}$; temperature, 20 °C; (a) Under argon, (b) under 1 atm of CO_2, (c) under 1 atm of CO_2, with 10 mM $Mg(ClO_4)_2$, −40 °C, (d) under argon, (e) under 1 atm of CO_2, (f) under 1 atm of CO_2 with 10 mM $Mg(ClO_4)_2$; working electrode, glassy carbon.

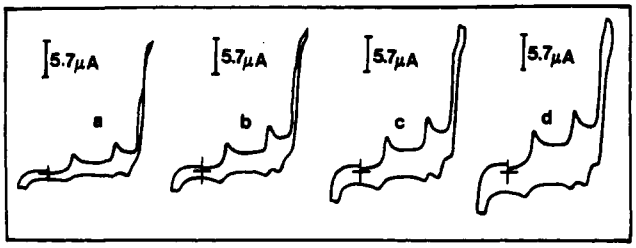

Figure 11. Cyclic voltammetry of TPPFeCl (0.5 mM) in DMF + 0.1 M NEt_4ClO_4 under 1 atm of CO_2 at −40 °C: scan rate ($V{\cdot}s^{-1}$) 0.1 (a), 0.2 (b), 0.3 (c), and 0.4 (d); working electrode, glassy carbon; potential scanning, 0.3 → −1.8 → 0.9 V vs SCE.

whereas, at 20 °C, reliable conclusions could only be reached when Mg^{2+} ions were present.

Figure 11 shows typical cyclic voltammograms obtained under 1 atm of CO_2 at −40 °C in the absence of Mg^{2+} ions as a function of the scan rate, whereas Figure 12 shows the effect of a variation of the CO_2 concentration. At low scan rates the catalytic wave is irreversible and has a plateau shape. Upon raising the scan rate it becomes slightly reversible and tends to take a peak shape. At all scan rates and CO_2 concentrations, the wave is split into two closely spaced waves. When it has a plateau shape, the total height of the wave is independent of the scan rate and proportional

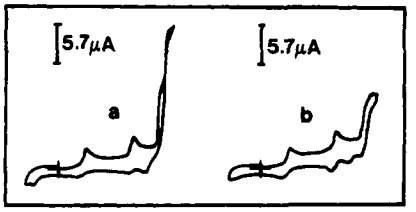

Figure 12. Cyclic voltammetry of TPPFeCl (0.5 mM) in DMF + 0.1 M NEt_4ClO_4 at 0.1 $V \cdot s^{-1}$: p_{CO_2} = 1 atm (a) and 0.5 atm (b): working electrode, glassy carbon; potential scanning 0.3 → −1.8 → 0.9 V vs SCE.

Scheme I

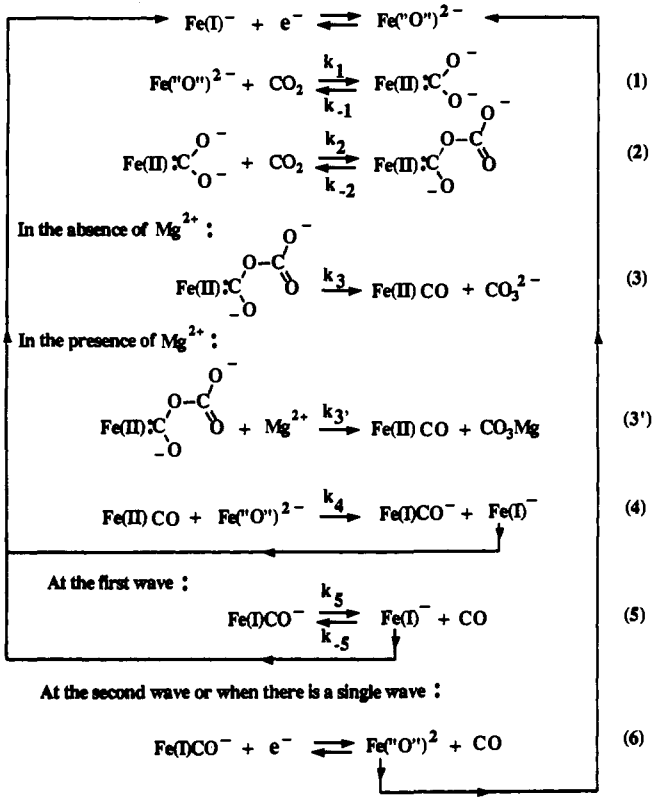

to the concentration of CO_2. Among the two closely spaced waves, all that increase the production of CO, namely a decrease of the scan rate and an increase of the CO_2 concentration, increase the first wave at the expense of the second.

These observations suggest the mechanism depicted in Scheme I. Since the concentration of CO_2 is very large compared to that of the catalyst and since the catalytic increase of the current is not very large, the consumption of CO_2 in the reaction-diffusion layer is negligible.[2c] It is thus expected, as observed experimentally, that the catalytic wave be irreversible with a plateau shape at low scan rate when pure kinetic conditions are met, i.e., when there is compensation between the diffusion of the reduced form of the catalyst and its reaction with the substrate.[2c,27] Then the height of the plateau, i_p, is given by[2c,27]

$$i_p = FSC^\circ D^{1/2}(k_{ap})^{1/2} \quad (1)$$

where S is the electrode surface area, D the diffusion coefficient of the catalyst, C° its bulk concentration, and k_{ap} is the apparent first-order rate constant globally characterizing the catalytic process. Alternatively[2c,27]

$$\frac{i_p}{i_p^\circ} = \frac{1}{0.446}\left(\frac{k_{ap}RT}{v\,F}\right)^{1/2} \quad (2)$$

where v is the scan rate and i_p° the peak height of any one-electrode reversible wave of the porphyrin catalyst.

It follows that the fact that the total plateau height is proportional to the CO_2 concentration indicates that the reaction order in CO_2 is 2. According to Scheme I

$$k_{ap} = K_1K_2k_3[CO_2]^2$$

where K_1 and K_2 are the equilibrium constants of steps 2 and 3. The observed CO_2 reaction order of 2 would also be consistent with a mechanism in which step 2 rather than step 3 would be rate-determining, i.e.

$$k_{ap} = 2K_1k_2[CO_2]^2$$

This second possibility is however ruled out by the analysis of the effects of the addition of Mg^{2+} ions as will be discussed later on. From the application of eq 2, it follows that

$$K_1K_2k_3 = 14\ M^{-2}\ s^{-1}$$

In Scheme I, we have represented the complexes resulting from the addition of one and then two molecules of CO_2 to the iron("0") porphyrin under the form of carbene complexes. These are only some of the possible resonant forms of these adducts among others. They however most probably have an important weight in view of the strong affinity of iron(II) porphyrins toward carbene including CO itself.[28] Upon addition of the first CO_2 molecule, electrons are shifted from the iron porphyrin to the CO_2 moiety. The second important step in the formation of CO, namely the breaking of one carbon–oxygen bond in the first CO_2 molecule entering the iron coordination sphere, is effected by the second CO_2 molecule which then acts as a Lewis acid similarly to the mechanism of the CO formation in direct electrolysis of CO_2 on inert electrodes.[3d] The $Fe^{II}CO$ complex then formed is much easier to reduce than the $Fe(I)^-$ complex. Since, in addition, the $Fe^{II}CO/Fe^{I}CO^-$ and $Fe(I)^-/Fe("0")^{2-}$ complex are intrinsically fast as revealed by cyclic voltammetry, reaction 4 in Scheme I is very fast, most probably close to the diffusion limit. The reduction of $Fe^{II}CO$ could also, in principle, take place at the electrode surface. However, this reaction is unlikely to compete with reaction 4 because with the catalytic reaction not being very fast, the $Fe^{II}CO$ complex is formed rather far from the electrode surface and will be reduced by the $Fe("0")^{2-}$ porphyrin before returning to the electrode surface.[29]

We interpret the splitting of the catalytic wave into two subwaves as being due to the complexation of the oxidized form of the catalyst, i.e., the iron(I) porphyrin by CO. This is much stronger at −40 °C than at 20 °C: the $Fe(I)^-/Fe("0")^{2-}$ reversible wave is shifted toward negative potentials by 56 mV at −40 °C, whereas there is no appreciable shift at 20 °C. This indicates, assuming as it seems quite probable that the $Fe("0")^{2-}$ porphyrin is not appreciably complexed by CO, that the $Fe^{I}CO^-/Fe(I)^-$ ratio

(27) (a) Savéant, J.-M.; Vianello, E. *Adv. Polarography* **1960**, 367. (b) Savéant, J.-M.; Vianello, E. *Electrochim. Acta* **1965**, *10*, 905. (c) Andrieux, C. P.; Dumas-Bouchiat, J.-M.; Savéant, J.-M. *J. Electroanal. Chem.* **1980**, *113*, 19. (d) Savéant, J.-M.; Su, K. B. *J. Electroanal. Chem.* **1984**, *171*, 341.

(28) (a) Caughey, W. S.; Maxwell, J. C.; Thomas, J. M.; O'Keefe, D. H.; Wallace, W. J. In *Metal Ligand Interaction in Organic Chemistry and Biochemistry, Part 2*; Pullman, B., Golblum, N., Eds., Reidel: Dordrecht, Holland, 1977, 131. (b) Wayland, B. B.; Mehne, L. F.; Swartz, J. *J. Am. Chem. Soc.* **1978**, *100*, 2379. (c) Lexa, D.; Savéant, J.-M.; Battioni, J. P.; Lange, M.; Mansuy, D. *Angew. Chem., Int. Ed. Engl.* **1981**, *20*, 578. (d) (132) Battioni, J. P.; Lexa, D.; Mansuy, D.; Savéant, J.-M. *J. Am. Chem. Soc.* **1983**, *105*, 207. (e) There is precedence for transition-metal complexes having two CO_2 molecules in their coordination sphere linked in the same way as in the present case.[10g] In the cited iridium complex, not only the first CO_2 molecule is coordinated to the metal through the carbon atom as here but also the second molecule is coordinated to the metal through one of its oxygen atoms unlike what we have represented in Scheme I. In iron porphyrins there are a few examples where some evidence has been provided for structures in which two atoms belonging to the same molecules are coordinated to the iron atom in a cis manner. They concern the binding at iron(III) porphyrins of doubly reduced dioxygen[28f] or of the percarbonate resulting from the inclusion of CO_2 in this complex.[28g] Such structures are less likely for iron(II) porphyrins where a carbene-type binding with a Fe–C bond perpendicular to the porphyrin ring seems in order. (f) Fischer, J.; Ricard, L.; Schappacher, M.; Weiss, R.; Momenteau, M. *Nouv. J. Chim.* **1985**, *9*, 33. (g) Schappacher, M.; Weiss, R.; Montiel-Montoya, R.; Trautwein, A.; Tabard, A. *J. Am. Chem. Soc.* **1985**, *107*, 3736.

(29) For a quantitative analysis of this type of competition see refs 2c, 27c, and 29b. (b) Savéant, J.-M.; Su, K. B. *J. Electroanal. Chem.* **1985**, *196*, 1.

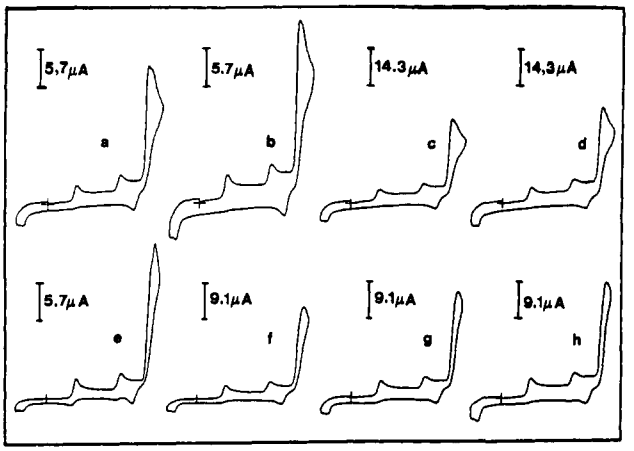

Figure 13. Cyclic voltammetry of TPPFeCl (0.5 mM) in DMF + 0.1 M NEt_4ClO_4 at a glassy carbon electrode in the presence of CO_2 and Mg^{2+} ions (2 mM) at −40 °C: potential scanning 0.3 → −1.9 → 0.9 V vs SCE.

	a	b	c	d	e	f	g	h
p_{CO_2} (atm)	0.5	0.5	0.5	0.5	1.0	1.0	1.0	1.0
v(V·s^{-1})	0.1	0.2	0.3	0.4	0.1	0.2	0.3	0.4

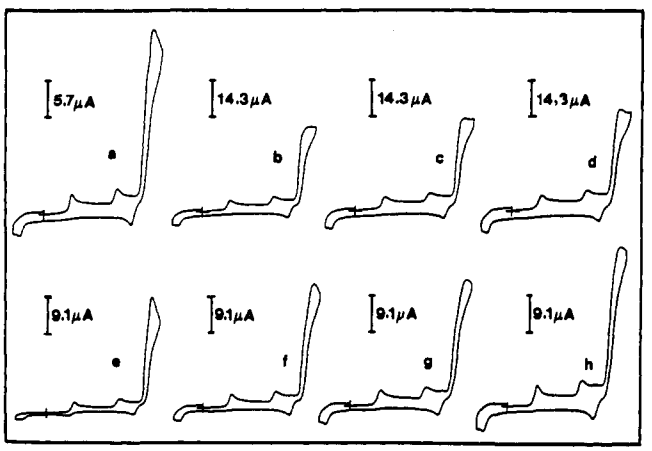

Figure 14. Cyclic voltammetry of TPPFeCl (0.5 mM) in DMF + 0.1 M NEt_4ClO_4 at a glassy carbon electrode in the presence of CO_2 and Mg^{2+} ions (4 mM) at −40 °C: potential scanning, 0.3 → −1.9 → 0.9 V vs SCE.

	a	b	c	d	e	f	g	h
p_{CO_2} (atm)	0.5	0.5	0.5	0.5	1.0	1.0	1.0	1.0
v(V·s^{-1})	0.1	0.2	0.3	0.4	0.1	0.2	0.3	0.4

is of the order of 20.[30] The first subwave thus corresponds to the regeneration of the oxidized form of the catalyst, i.e., the iron(I) porphyrin, through dissociation of the Fe^ICO^- complex, whereas the second subwave involves the direct reduction of Fe^ICO^- at a slightly more negative potential regenerating the catalyst under its reduced form (Scheme I). This interpretation is based on the observation that all factors that increase the production of CO (low scan rates, increase of CO_2 concentration) also increase the second subwave at the expense of the first. As discussed later on, this is confirmed by the effect of the Mg^{2+} ions and also by the fact that no splitting of the catalytic wave is observed at 20 °C where the complexation of the iron(I) porphyrin is very weak.

Typical examples of the effect of Mg^{2+} ions on the catalytic cyclic voltammetric waves are shown in Figures 13–15 for several values of the scan rate and of the concentration of CO_2. Many other concentrations of Mg^{2+} ions (9.8, 16, 22, 30, 40, 50, mM) were investigated. The most important facts that emerge from these experiments are as follows.

(30) (a) The solubility of CO in DMF is known at 20 °C and higher temperatures.[24b] It appears to decrease when the temperature is lowered and can be estimated to be 2 mM under 1 atm of CO at −40 °C. (b) The $Fe^ICO^-/Fe(I)^-$ ratio may well exceed 20 since the CO concentration in the reaction layer at low scan rate is likely to exceed 2 mM.

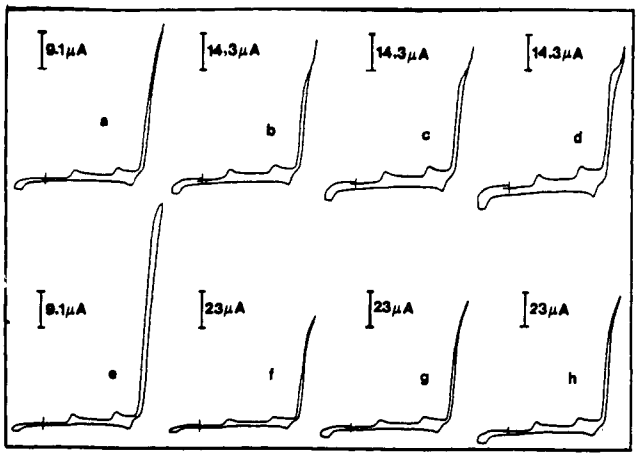

Figure 15. Cyclic voltammetry of TPPFeCl (0.5 mM) in DMF + 0.1 M NEt_4ClO_4 at a glassy carbon electrode in the presence of CO_2 and Mg^{2+} ions (16 mM) at −40 °C: potential scanning, 0.3 → −1.9 → 0.9 V vs SCE.

	a	b	c	d	e	f	g	h
p_{CO_2} (atm)	0.5	0.5	0.5	0.5	1.0	1.0	1.0	1.0
v(V·s^{-1})	0.1	0.2	0.3	0.4	0.1	0.2	0.3	0.4

Even at the lowest Mg^{2+} concentrations, the catalytic wave is higher and the production of CO (as measured by the changes in the $Fe(II)/Fe(I)^-$ and $Fe(II)/Fe(III)^+$ waves) is larger than in the absence of Mg^{2+} ions.

At a concentration of 16 mM in Mg^{2+} ions and above this value, there is a single catalytic plateau-shaped wave. The height of the plateau is independent of the scan rate and the concentration of Mg^{2+} and is proportional to the concentration of CO_2.

When the concentration of Mg^{2+} ions is smaller than 16 mM, the catalytic wave tends to split into two closely spaced subwaves as can be seen on Figures 13 and 14. At the lowest concentrations of Mg^{2+} ions (2 and 4 mM), the total wave becomes peak-shaped and the height of the peak decreases with the concentration of Mg^{2+} ions.

These observations provide evidence for the mechanism depicted in Scheme I. The breaking of one C–O bond in the first CO_2 molecules bound to the iron atom is accelerated by the Mg^{2+} ions (reactions 3′). Above 16 mM, the latter reaction is so fast that reaction 2 becomes the rate-determining step as indicated by the zero-order in Mg^{2+} ions and the second order in CO_2. This also demonstrates that, in the absence of Mg^{2+}, the rate-determining step was reaction 3 rather than reaction 2. Otherwise the introduction of Mg^{2+} ions would not have produced any acceleration of the catalytic reaction. Reaction 3′ is written as a single step in Scheme I. It might as well involve the intermediate formation of an Mg adduct such as the following.

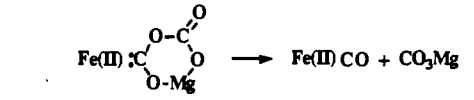

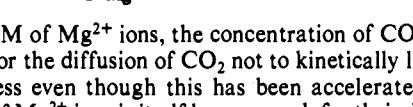

Above 16 mM of Mg^{2+} ions, the concentration of CO_2 is still large enough for the diffusion of CO_2 not to kinetically limit the catalytic process even though this has been accelerated. The concentration of Mg^{2+} ions is itself large enough for their diffusion not to limit the reaction. These are the reasons that the wave has a plateau shape and its height is independent from the scan rate. Equation 2 is thus again applicable, with

$$k_{ap} = 2K_1k_2[CO_2]^2$$

leading to

$$K_1k_2 = 250\ M^{-2}\ s^{-1}$$

For lower concentrations of Mg^{2+} ions, the kinetic control of the catalytic process passes progressively from reaction 2 to re-

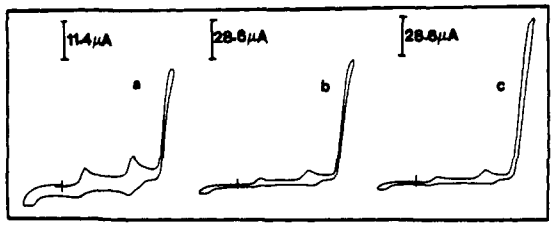

Figure 16. Cyclic voltammetry of TPPFeCl (0.5 mM) in DMF + 0.1 M NEt_4ClO_4 at 20 °C at a glassy carbon electrode under 1 atm of CO_2 in the presence of Mg^{2+} ions: Mg^{2+} concentration (mM) 3 (a), 24 (b), 68 (c); scan rate, 0.1 $V{\cdot}s^{-1}$; potential scanning, 0.3 → −1.9 → 0.9 V vs SCE.

action 3′. Simultaneously, the consumption of Mg^{2+} ions in the reaction-diffusion layer ceases to be negligible. The diffusion of Mg^{2+} ions then begins to interfere in the kinetic control, leading to peak-shape waves. This shows that the Mg^{2+} ions play the role of a cosubstrate (besides CO_2) rather than of a cocatalyst. Indeed, overall, Mg^{2+} ions are consumed in the reaction yielding CO_3Mg which is inactive in the breaking of the C–O bond of the CO_2 molecule bound to iron

$$2CO_2 + Mg^{2+} + 2e^- \rightarrow CO + CO_3Mg$$

Since the consumption of CO_2, the other substrate, remains negligible, the kinetics of the participation of Mg^{2+} ions in the catalytic process are formally the same as those of systems involving a single substrate, the consumption of which in the diffusion-reaction layer cannot be neglected.[31] The i_p/i_p° working curves previously derived[27c] for such systems can thus be applied in the present case, leading to the following estimate of the rate-limiting constant.

$$K_1K_2k'_3 = 5 \times 10^4\ M^{-3}\ s^{-1}$$

The remainder of the mechanism is the same as in the absence of Mg^{2+} ions (see Scheme I). Reaction 4 is fast and irreversible. As to the competition between reactions 5 and 6 giving rise to the splitting of the two waves, it follows the same rule as before: all that favors the production of CO favors pathway 6 at the expense of pathway 5. This is true, as before, not only for the effect of the scan rate and of the CO_2 concentration but also for that of Mg^{2+} ions. Within the range where the kinetics depend upon the Mg^{2+} concentration, its increase leads to an increase of the second subwave at the expense of the first (see, for example, Figures 13 and 14). Upon raising the Mg^{2+} concentration, the first subwave vanishes and the single wave observed at high Mg^{2+} concentration (16 mM and above) corresponds to pathway 6.

Let us now analyze the kinetics observed at 20 °C in the presence of Mg^{2+} ions. We first note that there is not a splitting of the catalytic wave, no matter what the concentrations of CO_2 and Mg^{2+} and the scan rate may be. A series of cyclic voltammetry experiments carried out varying the Mg^{2+} concentration showed that the catalytic wave is plateau-shaped except at the lowest Mg^{2+} concentrations (2–3 mM). Figure 16 shows typical examples of voltammograms thus obtained. Figure 17 summarizes the variation of the i_p/i_p° ratio with the CO_2 and Mg^{2+} concentrations. The fact that the catalytic wave is a single wave unlike what was observed at −40 °C is in full agreement with the observation that $Fe(I)^-$ is not detectably complexed by CO at 20 °C in contrast with the observations, made at −40 °C. The regeneration of the catalyst thus entirely takes place through reaction 5 which converts the $Fe^{I}CO^-$ initially formed into the oxidized form, Fe(I) of the catalyst. Another important difference is that the order in Mg^{2+} ions is 1 with a slight tendency to decrease at high Mg^{2+} concentrations (Figure 17a). The zero order in Mg^{2+} found at −40 °C above 16 mM is not found here, up to concentrations as high as 74 mM. On the other hand, the reaction order in CO_2 is 1 (Figure 17b) as opposed to the reaction order of 2

(31) This equivalence can readily be proven in a rigorous manner at the level of the partial derivative equations, initial and boundary conditions that govern the system.

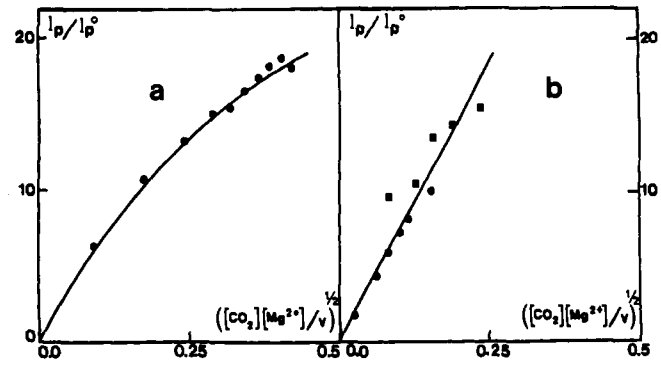

Figure 17. Cyclic voltammetry of TPPFeCl (0.5 mM) in DMF + 0.1 M NEt_4ClO_4 at 20 °C at a glassy carbon electrode in the presence of CO_2 and Mg^{2+} ions. Variations of the i_p/i_p° ratio with the parameter $([CO_2][Mg^{2+}]/v)^{1/2}$ (a) p_{CO_2} 1 atm, from left to right, $[Mg^{2+}]$ (mM) = 2, 12, 24, 36, 42, 49, 56, 62, 68, 74; (b) (●) $[Mg^{2+}]$ = 10 mM, from left to right, $[CO_2]$ (mM) = 10, 42, 70, 100, 140, 235; (■) $[Mg^{2+}]$ = 24 mM, from left to right, $[CO_2]$ (mM) = 24, 69, 103, 152, 235; scan rate, 0.1 $V{\cdot}s^{-1}$.

Scheme II

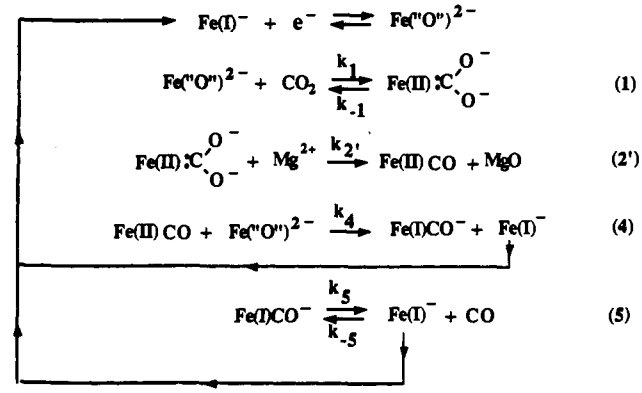

found at −40 °C in the presence and absence of Mg^{2+} ions. These facts suggest the mechanism depicted in Scheme II. The exact manner in which the Mg^{2+} ions break the C–O bond in the iron complex containing a single molecule of CO_2 is not known with certainty. It could be a direct reaction yielding MgO in a first step as represented in Scheme II. In such a case, MgO would be converted into CO_3Mg by reaction with excess CO_2. However, it could as well involve the formation of an Mg adduct such as

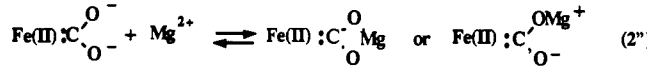

and, in a second step, its decomposition into $Fe^{II}CO$ and MgO. One could even invoke the possibility that this decomposition would involve, after addition of a second CO_2 molecule, the intermediacy of the complex:

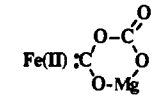

whose formation was evoked in the discussion of the mechanism taking place at −40 °C. In such a mechanism, the rate-determining step should be reaction 2″ otherwise the reaction order in CO_2 would be 2 instead of 1. We note, incidentally, that the mechanism depicted in Scheme II does not fit the kinetic data obtained at −40 °C. In the present mechanism indeed, an increase of the Mg^{2+} concentration leads necessarily to a reaction order in CO_2 equal to 1 and not to 2 as observed experimentally. Whatever the intimate mechanism of the C–O bond breaking by CO_2, application of eq 2 to the present case with

$$k_{ap} = 2K_1k_{2'}$$

leads to

$$K_1k_{2'} = 7 \times 10^5\ M^{-2}\ s^{-1}$$

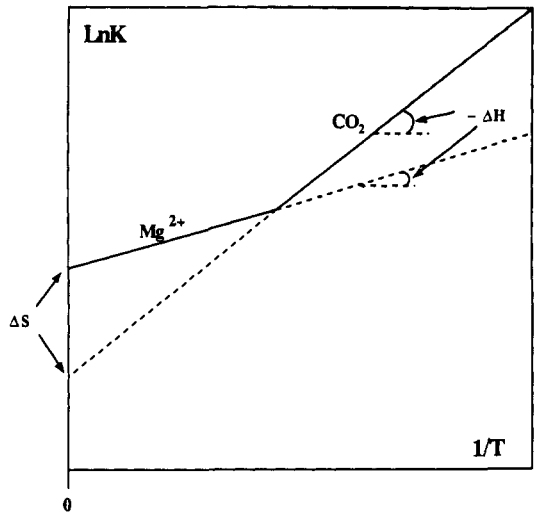

Figure 18.

The comparison of the kinetics of the reaction at 20 °C and −40 °C thus indicates that reaction 2″ is faster than reaction 2 at 20 °C, whereas the competition is inverted at −40 °C. Taking account of the range of CO_2 and Mg^{2+} concentrations within which the experiments were carried out one concludes that $k''_2 < 100k_2$ at 20 °C and $k''_2 > 1000k_2$ at −40 °C. In other words, the rate constant of reaction 2 decreases less rapidly with temperature than that of reaction 2″. If we assume that these variations are mainly due to different variations of the driving forces of the two reactions with temperature rather than variations in their instrinsic barriers, this would mean that the equilibrium constant of reaction 2 increases more rapidly upon decreasing the temperature than does that of reaction 2″. A likely situation in terms of van't Hoff plots in this connection is that represented in Figure 18. In the association of Mg^{2+} ions with the Fe^{II}:$C(O^-)O^-$ complex, as in most ion-pairing reactions, the reaction entropy plays a major role. Mg^{2+} ions are strongly associated with DMF molecules because of their Lewis base character. The enthalpy of reaction is thus not very favorable to association, being slightly negative (as represented in Figure 18) or possibly slightly positive. In contrast, the reaction entropy is positive because of the breaking of Mg^{2+}–solvent interactions. CO_2 molecules are also associated with DMF molecules but to a lesser extent than Mg^{2+} ions. The enthalpy of association is thus expected to be more negative and the entropy less positive, as represented in Figure 17. Under such conditions, the ratio of the equilibrium constants of reactions 2″ and 2 decreases upon decreasing the temperature. It is thus conceivable, taking account of the differences in concentration of Mg^{2+} ions and CO_2, that reaction 2″ predominates over reaction 2 at 20 °C and vice versa at −40 °C.

Concluding Remarks

The main conclusions emerging from the above results and discussions are the following. Iron("0") porphyrins do catalyze the electrochemical reduction of carbon dioxide. The main reduction product is carbon monoxide. However, the porphyrin is rapidly consumed, and the catalysis stops after a small number of cycles. The degradation of the porphyrin appears to be the result of progressive saturation of the ring through carboxylation and/or hydrogenation. As compared with TPP, superstructured porphyrins containing secondary amide groups last a little longer and give rise to better faradaic yields in CO. However, these improvements remain modest. The addition of Mg^{2+}, in the form of a nonhydrated salt with a nonnucleophilic (or weakly nucleophilic) counteranion such as perchlorate, triggers a spectacular increase in the catalytic efficiency and the stability of the catalyst. These improvements are best achieved with the simple TPP, whereas the superstructured porphyrins investigated continue to be consumed in the catalytic reaction albeit to a lesser extent than without Mg^{2+} ions in solution. Lewis acids such as LiCl, $BaCl_2$, and $AlCl_3$ also improve the catalytic efficiency and the stability of the catalyst but to a much lesser extent than "free" (although complexed by solvent molecules) Mg^{2+} ions.

Decreasing the temperature increases the catalytic efficiency mostly because CO_2 is more soluble. The fact that this effect is not compensated by a decrease of the rate-determining kinetic constant indicates that the overall reaction possesses a small activation energy. The degradation of the porphyrin also appears to be lowered upon decreasing the temperature.

The comparison with homogeneous catalysis by outer-sphere electron donors (benzonitrile anion radicals and similar nitriles or esters) clearly indicates that iron("0") porphyrins act as chemical rather than redox catalysts in the reduction of CO_2: the main product is different (CO instead of oxalate) and the catalytic efficiency is higher for the same standard potential of the catalyst couple.

At low temperature (−40 °C) as well as at room temperature (20 °C), the catalytic process begins with the introduction of one molecule of CO_2 in the coordination sphere of the iron atom (Schemes I and II) forming a carbene-type complex in which electrons have been transferred from the iron porphyrin to the CO_2 moiety. At low temperature, the second step, in the absence as well as in the presence of Mg^{2+} ions, is the addition of a second molecule of CO_2 in an acid–base-type manner. The C–O bond of the first CO_2 molecule is then broken with formation of the $Fe^{II}CO$ complex and of a carbonate ion. This reaction is accelerated by the presence of Mg^{2+} ions, presumably through the intermediary formation of a magnesium complex. At room temperature, the Mg^{2+} ions participate earlier to the breaking of the C–O, namely at the level of the first iron–CO_2 adduct. This variation of the reaction pathway with temperature falls in line with the expected differences in the entropy–enthalpy balance for the formation of an ion-pair with a Mg^{2+} ion on one hand and the addition of a CO_2 molecule on the other, taking into account the interactions of these two species with the solvent.

At room temperature the coordination of CO with the iron(I) porphyrin is weak, and the oxidized form of the catalyst, i.e., the iron(I) porphyrin, is regenerated without difficulty. This is not the case at low temperature where the dissociation of the Fe^ICO^- complex is more difficult. The regeneration of the catalyst thus follows the above pathway only in part, the remainder of the Fe^ICO^- porphyrin being reduced at a slightly more negative potential thus regenerating the catalyst in its reduced form.

The role played by the Mg^{2+} ions in the catalytic reaction offers a noteworthy example of a bimetallic chemical catalysis of an electrochemical reduction where an electron-rich center, here the iron("0") porphyrin, commences the reduction process in an inner-sphere fashion and an electron-poor center, here a Mg^{2+} ion, completes the bond transformation process in a manner that is reminiscent of electrophilic assistance in nucleophilic substitution. It should however be noted that Mg^{2+} ions play the role of a cosubstrate rather than that of a cocatalyst.

With regards to the electron(s) donor properties of iron("0") porphyrins, previous studies have shown that the iron center plays the role of a nucleophile toward carbon- or halogen-centered electrophiles. This is confirmed by the present work in the case of CO_2. However, the rapid deactivation of the catalyst at room temperature in the absence of Mg^{2+} ions also shows that some of the electron density introduced upon reduction of the iron(I) porphyrin is present on the porphyrin ring allowing its carboxylation and/or hydrogenation in competition with the chemistry taking place at the iron center. The latter is greatly favored by electrophilic assistance. This however requires the use of hard electrophiles that must possess at the same time a strong Lewis acidity and a low electron affinity. Decreasing the temperature is also a favorable factor because it facilitates the introduction of the substrate into the coordination sphere of the metallic center.

Experimental Section

Chemicals. DMF from commercial origin (Carbo, Erba, Merck) was distilled over barium oxide under nitrogen at reduced pressure at 50° before use. The tetraethylammonium perchlorate, Fluka puum was recrystallized thrice in a 2:1 ethanol–ethyl acetate mixture and then dried under vacuum at 50 °C. $Mg(ClO_4)_2$, LiCl, $BaCl_2$, $AlCl_3$, and TPPFeCl

were obtained from Aldrich and used as received. The a-PF and a-$(Cl2)_2$-CT-TPPFeCl porphyrins were synthesized as described in ref 32. CO_2 was of N45 grade from Alphagas (Air Liquide).

Cyclic Voltammetry and Thin-Layer UV-vis Spectroelectrochemistry. The cells, instruments, and procedures used for cyclic voltammetry and thin-layer UV-vis spectroelectrochemistry were the same as previously described.[33] The UV-vis spectra were recorded on a Varian 2300 spectrophotometer. The working electrodes were a 3-mm diameter glassy carbon disk (frequently polished with diamond pastes down to 1 μm) or a mercury drop hung onto a gold disk in cyclic voltammetry and a 2.4 cm^2 platinum grid in spectroelectrochemistry. The reference electrode was a NaCl saturated calomel electrode. Dilution of CO_2 with argon was carried out by means of a mass flow regulator (Air liquide Alphagaz) allowing a constant partial pressure of CO_2 to be established.

Preparative Scale Electrolysis Product Analysis. We used a gas-tight cell allowing the CO_2 pressure to remain constant during the electrolysis similar to that described in ref 131. The mercury pool cathode was vigorously agitated by means of a magnetic stirrer. A platinum wire separated from the cathodic compartment by a Nafion membrane or a magnesium wire were used as anodes. The reference electrode was again a NaCl saturated calomel electrode. After saturation of the solution during 30 min by CO_2 dried over a $CaCl_2$ or silica gel column, the cell was isolated. The first electrolysis was carried out at the potential where the Fe(III) porphyrin is converted into its Fe(II) form. A second electrolysis was then performed at the potential where the Fe(II) porphyrins is converted into its Fe(I) form. These two preliminary electrolyses lasted about 10 min each. The potential was then set to the value where the catalysis takes place, i.e., the potential where the Fe(I) porphyrins are converted into the Fe("0") form. The electrolysis was pursued up to about 4 h. We assayed for CO and H_2 by means of gas chromatography on silica gel or Porapak columns. Formaldehyde was looked for by means of the chromotropic acid method.[34a] The same method was used for testing the possible presence of formate, after reduction of the acidified solution by magnesium.[34b] For testing the possible presence of oxalate we carried out a series of electrolyses in *n*-butyronitrile with *n*-Bu_4NClO_4 as supporting electrolyte. By using *n*-butyronitrile, which is unmiscible with water we could extract the oxalate ions from the organic phase and titrate them in the aqueous extract with a saturated solution of $BaCl_2$. The production of CO in these electrolyses was essentially the same as in the electrolyses carried out in DMF.

Acknowledgment. We are indebted to Prof. Elio Vianello (Padova, Itay) for the communication of his results on the redox catalysis of the electrochemical reduction of CO_2[2e] prior to publication.

(32) (a) Collman, J. P.; Gagne, R. R.; Reed, C. A.; Malbert, T. R.; Lang, G.; Robinson, W. T. *J. Am. Chem. Soc.* **1975**, *97*, 1427. (b) Momenteau, M.; Mispelter, J.; Loock, B.; Lhoste, J. M. *J. Chem. Soc., Perkins Trans. 1* **1985**, 221. (c) Momenteau, M.; Loock, B. *J. Mol. Catal.* **1980**, *7*, 315. (d) Momenteau, M.; Mispelter, J.; Loock, B.; Bisagni, E. *J. Chem. Soc., Perkins Trans 1* **1983**, 189.

(33) Lexa, D.; Savéant, J.-M.; Zickler, J. *J. Am. Chem. Soc.* **1977**, *99*, 786.

(34) (a) Grant, W. M. *Anal. Chem.* **1948**, *20*, 267. (b) Bricker, C. E.; Vail, W. A. *Anal. Chem.* **1950**, *22*, 720.

Ruthenium/Zirconium Complexes Containing C_2 Bridges with Bond Orders of 3, 2, and 1. Synthesis and Structures of $Cp(PMe_3)_2RuCH_nCH_nZrClCp_2$ (n = 0, 1, 2)

Frederick R. Lemke,[†] David J. Szalda,[‡] and R. Morris Bullock*

Contribution from the Department of Chemistry, Brookhaven National Laboratory, Upton, New York 11973. *Received March 4, 1991*

Abstract: A series of Ru/Zr complexes linked by C_2 bridges of bond orders 3, 2, and 1 were prepared, and characterized by spectroscopic data and single-crystal X-ray diffraction. The dimetalloalkyne complex $Cp(PMe_3)_2RuC{\equiv}CZrClCp_2$ was prepared by the reaction of $Cp(PMe_3)_2RuC{\equiv}CH$ with either $Cp_2Zr(CH_3)Cl$ or $Cp_2Zr(NMe_2)Cl$. This dimetalloalkyne is the first example of a structurally characterized alkyne that is substituted by an electron-rich metal at one end, and by an electron-deficient metal at the other. The reaction of $Cp(PMe_3)_2RuC{\equiv}CH$ with $[Cp_2Zr(H)Cl]_n$ gives the dimetalloalkene complex $Cp(PMe_3)_2RuCH{=}CHZrClCp_2$, which has a three-center, two-electron agostic interaction between the Zr and the vinylic CH that is β to Zr. Carbonylation of $Cp(PMe_3)_2RuCH{=}CHZrClCp_2$ with 1 atm of CO produces the η^2-acyl complex $Cp(PMe_3)_2RuCH{=}CHC(O)ZrClCp_2$. Analysis of the spectroscopic and structural data for this acyl compound indicates a substantial contribution from a zwitterionic resonance form that has a formal positive charge at Ru and a negative charge on the Zr portion. Hydrolysis of $Cp(PMe_3)_2RuCH{=}CHZrClCp_2$ produces the known zirconium complex $[Cp_2ZrCl]_2O$ and the ruthenium vinyl complex $Cp(PMe_3)_2RuCH{=}CH_2$. Reaction of $[Cp_2Zr(H)Cl]_n$ with $Cp(PMe_3)_2RuCH{=}CH_2$ gives the dimetalloalkane complex $Cp(PMe_3)_2RuCH_2CH_2ZrClCp_2$. Spectroscopic and crystallographic data are interpreted to indicate that this compound also has an agostic interaction between the Zr and a CH adjacent to Ru.

Organometallic complexes in which two or more metals are linked by a hydrocarbon bridge have been studied extensively as models for species postulated to be present in several important metal-catalyzed reactions.[1] Detailed investigations of the ways in which metal-carbon and carbon-carbon bonds are made and broken in these soluble complexes can provide useful information for comparison to similar processes that occur in homogeneous catalytic reactions and on metal surfaces. Methylene-bridged complexes are a thoroughly investigated class of C_1-bridged complexes.[2] Most methylene-bridged complexes contain identical or similar metals bonded to the $-CH_2-$ bridge. Methylene-bridged complexes in which the $-CH_2-$ bridge links two metals of disparate electronic properties, though relatively rare, have proven to exhibit

[†] Present address: Department of Chemistry, Ohio University, Athens, OH 45701-2979.

[‡] Research Collaborator at Brookhaven National Laboratory. Permanent address: Department of Natural Sciences, Baruch College, New York, NY 10010.

(1) For reviews of organometallic hydrocarbon-bridged complexes, see: (a) Casey, C. P.; Audett, J. D. *Chem. Rev.* **1986**, *86*, 339-352. (b) Holton, J.; Lappert, M. F.; Pearce, R.; Yarrow, P. I. *Chem. Rev.* **1983**, *83*, 135-201. (c) Moss, J. R.; Scott, L. G. *Coord. Chem. Rev.* **1984**, *60*, 171-190.

(2) For a review of methylene-bridged complexes, see: Herrmann, W. A. *Adv. Organomet. Chem.* **1982**, *20*, 159-263. For a review of methylene-bridged complexes without metal-metal bonds, see: Puddephatt, R. J. *Polyhedron* **1988**, *7*, 767-773.

0002-7863/91/1513-8466$02.50/0